Published in final edited form as:
Pulm Circ. 2011 January 1; 1(1): 48–71. doi:10.4103/2045-8932.78103.

Functional ion channels in human pulmonary artery smooth muscle cells: Voltage-dependent cation channels

Amy L. Firth[1], **Carmelle V. Remillard**[2], **Oleksandr Platoshyn**[2], **Ivana Fantozzi**[2], **Eun A. Ko**[3], and **Jason X.-J. Yuan**[2,3]

[1]The Salk Institute for Biological Studies, La Jolla, California, USA

[2]Department of Medicine, University of California, San Diego, La Jolla, California, USA

[3]Department of Medicine (Section of Pulmonary, Critical Care, Sleep and Allergy), Institute for Personalized Respiratory Medicine, University of Illinois at Chicago, Chicago, Illinois, USA

Abstract

The activity of voltage-gated ion channels is critical for the maintenance of cellular membrane potential and generation of action potentials. In turn, membrane potential regulates cellular ion homeostasis, triggering the opening and closing of ion channels in the plasma membrane and, thus, enabling ion transport across the membrane. Such transmembrane ion fluxes are important for excitation-contraction coupling in pulmonary artery smooth muscle cells (PASMC). Families of voltage-dependent cation channels known to be present in PASMC include voltage-gated K^+ (Kv) channels, voltage-dependent Ca^{2+}-activated K^+ (Kca) channels, L- and T- type voltage-dependent Ca^{2+} channels, voltage-gated Na^+ channels and voltage-gated proton channels. When cells are dialyzed with Ca^{2+}-free K^+- solutions, depolarization elicits four components of 4-aminopyridine (4-AP)-sensitive Kvcurrents based on the kinetics of current activation and inactivation. In cell-attached membrane patches, depolarization elicits a wide range of single-channel K^+ currents, with conductances ranging between 6 and 290 pS. Macroscopic 4-AP-sensitive Kv currents and iberiotoxin-sensitive Kca currents are also observed. Transcripts of (a) two Na^+ channel α–subunit genes (SCN5A and SCN6A), (b) six Ca^{2+} channel α–subunit genes (α_{1A}, α_{1B}, α_{1x}, α_{1D}, α_{1E} and α_{1G}) and many regulatory subunits ($\alpha_2\delta_1$, $\beta_{1\text{-}4}$, and γ_6), (c) 22 Kv channel α–subunit genes (Kv1.1 - Kv1.7, Kv1.10, Kv2.1, Kv3.1, Kv3.3, Kv3.4, Kv4.1, Kv4.2, Kv5.1, Kv 6.1-Kv6.3, Kv9.1, Kv9.3, Kv10.1 and Kv11.1) and three Kv channel β-subunit genes (Kv(β1-3) and (d) four Kca channel α–subunit genes (*Slo*α1 and SK2-SK4) and four Kca channel (β-subunit genes (Kca(β1-4) have been detected in PASMC. Tetrodotoxin-sensitive and rapidly inactivating Na^+ currents have been recorded with properties similar to those in cardiac myocytes. In the presence of 20 mM external Ca^{2+}, membrane depolarization from a holding potential of -100 mV elicits a rapidly inactivating T-type Ca^{2+} current, while depolarization from a holding potential of -70 mV elicits a slowly inactivating dihydropyridine-sensitive L-type Ca^{2+} current. This review will focus on describing the electrophysiological properties and molecular identities of these voltage-dependent cation channels in PASMC and their contribution to the regulation of pulmonary vascular function and its potential role in the pathogenesis of pulmonary vascular disease.

Address correspondence to: Prof. Jason X.-J. Yuan, Department of Medicine (Section of Pulmonary, Critical Care and Sleep and Allergy), Institute for Personalized Respiratory Medicine, University of Illinois at Chicago, COMRB Rm. 3131 (MC 719), 909 South Wolcott Avenue, Chicago, Illinois 60612, USA, jxyuan@uic.edu.

Conflict of Interest: None declared.

Keywords

Ca^{2+} channel; K^+ channel; membrane potential; Na^+ channel; pulmonary hypertension

Introduction

Intracellular ion homeostasis, cell volume and membrane excitability are all important mechanisms regulated by the membrane permeability to cations and anions. It is this transmembrane ion flux that is the predominant factor in controlling excitation–contraction (EC) coupling mechanisms in pulmonary artery smooth muscle cells (PASMC). Electromechanical and pharmacomechanical coupling processes are the two major EC coupling mechanisms. Of these, it is the electric excitability that plays an important role in EC coupling in the pulmonary vasculature,[1,2] predominantly controlled by the transmembrane ion flux in PASMC. Indeed, many vasoactive substances also alter the membrane potential (E_m) in these cells.[3,4] Expression and functionality of ion channels in the plasma membrane is also important in modulation of cell motility, migration and proliferation by governing the cytoplasmic free Ca^{2+} concentration ($[Ca^{2+}]_{cyt}$).

A rise in $[Ca^{2+}]_{cyt}$ in PASMC triggers pulmonary vasoconstriction[5] and stimulates cell proliferation[6] and migration,[7] leading to pulmonary vascular remodeling.[8] The mechanisms involved in the regulation of $[Ca^{2+}]_{cyt}$ directly control vasomotor tone and vascular wall thickness; two major determinants of pulmonary vascular resistance (PVR). Because PVR is inversely proportional to the fourth power of the radius (r) of the pulmonary arterial lumen ($PVR=8L\eta/\pi r^4$), a very small change in r would thus cause a large change in PVR. As a consequence, pulmonary vasoconstriction will also increase PVR by reducing the arterial radius. Pulmonary arterial pressure (PAP), a diagnostic criterion for PAH, is a product of PVR and cardiac output. Pulmonary vasoconstriction and vascular medial hypertrophy caused by excessive PASMC proliferation and migration contribute considerably to the elevated PVR in patients with pulmonary hypertension. Indeed, dysfunction of a number of ion channels has been implicated in a variety of cardiopulmonary diseases, such as pulmonary arterial hypertension,[8,9] spontaneous genetic systemic arterial hypertension[10-13] and heart failure.[14] Therefore, defining the molecular identities and electrophysiological properties of plasmalemmal ion channels in human PASMC will help to enhance our understanding of normal EC coupling mechanisms, to define the pathogenic roles of ion channels in pulmonary vascular disease and to develop new therapeutic approaches for patients with pulmonary hypertension.

As mentioned above, EC coupling requires a change in membrane potential to alter vascular tone. Ion channels are sarcolemmal pores selectively permeable to either cations (Na^+, Ca^{2+}, K^+) or anions (Cl^-). Both anions and cations are distributed on either side of the cell membrane, and their transmembrane movement is based on their electrochemical gradient, a potential- and concentration-based driving force for the ions, i.e. flowing from more-concentrated to less-concentrated zones and, for cations, from positive or less-negative sites to those with a more negative membrane potential. In human cells, Na^+ (~140 mM) and Ca^{2+} (~2 mM) are the dominant cations in the external fluid (concentrations similar to those found in blood plasma), whereas K^+ (~140 mM) is the dominant cation in the cell cytoplasm. Cl^-, the most dominant anion in vascular smooth muscle cells,[15] is unevenly distributed between the cytosol and the extracellular fluids, and plays an important role in controlling osmolarity, cell volume, excitability and ion homeostasis [Table 1]. Additionally, ion channels expressed in the plasma membrane also play important roles in the regulation of secretion, migration, proliferation, differentiation and apoptosis. In vascular smooth muscle cells, the resting E_m is predominantly regulated by the permeability

and the concentration gradients of K^+ across the plasma membrane. The reason that the resting E_m (-40 to -55 mV) in vascular smooth muscle cells is not equal to the K^+ equilibrium potential (approximately -85 mV) indicates that other cation (e.g., Na^+ and Ca^{2+}) and anion (e.g., Cl^-) channels also contribute to regulating the E_m. This review will provide an in-depth summary of the molecular identities and electrophysiological properties of voltage-dependent cation channels in PASMC, focusing on Na^+ and Ca^{2+} channels, which are opened by membrane depolarization and responsible for cell excitation, and voltage-gated Kv and Kca channels, which are responsible for controlling resting E_m and repolarization when the cells are stimulated.

Passive cell membrane properties of human PASMC

The whole-cell patch clamp configuration[16] may be likened to an electrical circuit [Figures 1 and 2a]. A capacitor is made with two charged surfaces separated by a dielectric substance. The pipette itself is such a dielectric substance with two charged surfaces and, therefore, is represented by a capacitor in the circuit. Pipette capacitance (C_p, measured in Farads, F) is complicated in character, but its contribution to the overall circuit is usually minimized electronically by injecting a current transient designed to pre-charge the glass surface to the new desired potential. The pore of the pipette presents a resistance to current flow that may be easily measured before seal formation (R_e, measured in Ohms, Ω). During whole-cell access, however, this resistance is increased by further resistance to current flow due to the contents or geometry of the cell itself ("series resistance" or "access resistance," R_a), i.e. resistance to filling the entire cytosolic space with the desired amount of charge or potential due to interaction of charges with proteins or due to limited flux through long cell processes or narrow cell geometry.

Once the cytosolic space of the cell is voltage clamped, the cell membrane also presents its own capacitance. Unlike the pipette, the cell membrane is of relatively uniform thickness and uniform dielectric content (lipids); therefore, in most cells, the specific membrane capacitance (C_m), which is normalized by the area of the plasma membrane, is ~1 μF/cm^2,[17] and a measure of the cell capacitance is a good indicator of cell size. The cell membrane itself is a very good dielectric, presenting a resistance of several gigaOhms (gigaΩ) when the membrane channels are closed at rest, in effect stopping the flow of charge across the membrane. However, the membrane resistance (R_m) is strongly influenced by the presence of ion conductances through the membrane ion channels.

Ion channels are selectively permeable to specific cations, and have a gating mechanism that may be controlled by voltage or other methods. Ion channels produce a conductance (g, measured in Siemens, S) that is dependent on the transmembrane electrical potential energy (ΔE, or E_m, measured in Volts, V), and defined by Ohm's law, I_x=gE, where I_x is the conductance or current through that particular type of channel. Because Ohm's law defines resistance as the inverse of conductance, the overall membrane resistance is the inverse of the sum of all the conductances present on the membrane. The simple measurement of overall membrane resistance is therefore a good indicator of the amount of current carried through all the open channels on the membrane. As many membrane channels are voltage dependent, the membrane resistance likewise varies with membrane potential.

By employing a small hyperpolarizing command voltage step (V_{comm}), for example from -70 mV to -85 mV (close to the equilibrium potential for K^+), current transient (I_{tran}) is induced [Figure 2b]. The cell membrane capacitance (C_m) can then be determined by pClamp software based on the equation: C_m=(integral of I_{tran})/)V_{comm}). The membrane input resistance (R_m) is then calculated from the equation: $R_m=(R_{total}\times R_{seal})/(R_{seal}-R_{total})$, where R_{seal} and R_{total} are the resistance determined, respectively, from the steady currents of I_{tran} in response to V_{comm} (-5 mV) before and after break-in. As shown in Figure 2c, C_m can range

from 15 pF to 45 pF, with an average C_m of 34±5 pF measured in 220 PASMC. The specific membrane capacitance can be calculated from the mean values of C_m and cell surface (capacitative) area; for PASMC, this is in the region of 1.25 μF/cm^2, similar to the 1.3 μF/cm^2 reported in rat caudal artery smooth muscle cells.[18] R_m under resting conditions is usually very high in the vascular smooth muscle cells.[19] Indeed, the calculated R_m in PASMC ranges from 1 GΩ to 12 GΩ, with an average R_m of 5±1 GΩ (n=171) [Figure 2d]. Importantly, the duration of PASMC in cell culture conditions does not significantly alter the values for C_m and R_m [Figure 2e and f].

Membrane potential can be measured in the current-clamp (I=0) mode. The resting E_m in cultured human PASMC is approximately -45±5 mV [Figure 3a], and is slightly less negative than that observed in freshly dissociated PASMC from animals [20,21] As previously mentioned, E_m is less negative than the E_K (approximately -85 mV), which suggests that E_m in these cells is also controlled by the permeability of other ions (e.g., Na^+, Ca^{2+} and Cl^-). The equilibrium potentials for Na^+, Ca^{2+} and Cl^- are believed to be +66, +122 and -26 mV, respectively, in native vascular smooth muscle cells.[15] In some PASMC, spontaneous electrical activity has been observed under resting conditions [Figure 3b], suggesting that these cells are electrically excitable.[22] This spontaneous electrical activity in PASMC is dependent upon the presence of extracellular Ca^{2+} [Figure 3b].[2,23-25]

Evolution and diversity of the pore-forming voltage-gated cation channels

Ion-selective voltage-gated cation channels generate electrical activity in cells by undergoing rapid conformational changes from an impermeable structure to a highly permeable pore in the membrane through which ions can pass. Based on inherent similarities in the transmembrane domain structure of Na^+, Ca^{2+} and K^+ channel pore-forming α subunits, it is widely agreed upon that voltage-gated cation channels share a common ancestor. The basic building block of all these channels is a one-domain (1D) two-transmembrane segment (2TM) protein with an ion-selective pore/loop region between the transmembrane segments,[26] reminiscent of prokaryotic and eukaryotic K^+-selective inward rectifier channels [Figure 4]. Indeed, K+ channels are the oldest of the voltage-gated cation channels as examples of these have been found in both prokaryotic and eukaryotic organisms.[27] Over time, multiple gene duplications and modifications elaborated this channel by the addition of four transmembrane segments, forming 1D six-transmembrane segment (6TM) protein that constitutes the basic pore-forming α–unit of mammalian voltage-gated cation channels. From this point, the evolution of voltage-gated ion channels diverged, with ion selectivity being a key element to channel diversification. Figure 4 provides a simple phylogenetic tree of voltage-gated cation channels based on sequence identity and domain arrangement.

K^+ channels evolved into the most diverse family of channels, mainly due to the sheer number of α–subunits and possible $\alpha_4\beta_4$ subunit combinations. Four superfamilies of human K^+ channels have maintained the 1D-6TM motif, and multiple α–subunits have surfaced for each: *ether-a-go-go* (*eag*, *erk*, *elk*; 3 isoforms in human), KQT (5 isoforms in humans), Kca (maxi-Kca and SKca; 6 isoforms in humans) and Kv (11 subfamilies and ≥30 isoforms) (see Coetzee *et al.* for review[28]). The sequence identity varies greatly within (e.g., 35–88% identity between Kv1 and Kv9) and between (e.g., 8–17% identity between Kv and Kca) the families.[28] Chromosomal site analysis of the known human isoforms also suggests that K^+ channels have existed for a long time. Genes encoding 1D-6TM K^+ channels are found on at least 13 human chromosomes, with little evidence of clustering of genes except in the case of a few Kv channels (Figure 5 depicts the chromosomal location of channel pore-forming and regulatory subunits identified in human PASMC). Kv channel α–subunits alone can be found on 10 chromosomes within the human genome.

Na^+ and Ca^{2+} channels evolved after K^+ channels were well established.[27] A few theories have been put forth to explain the development of four-domain (4D) -6TM channels from 1D-6TM channels:[26] (a) two rounds of gene duplication of 1D-6TM K+ channels (1D÷2D, 2D÷4D) and mutations within the pore region to alter ion selectivity created the 4D-6TM Ca^{2+} and Na^+ channels.[26] Coupled with mutations within the pore to alter ion selectivity, this evolutionary cascade would have produced the 4D-6TM Ca^{2+} and Na^+ channels. (b) 1D- and 4D-6TM channels have a common 1D-6TM cyclic-nucleotide gated (CNG) channel ancestor, with S4 and pore regions similar to voltage-gated K^+, Ca^{2+} and Na^+ channels. In addition to structural similarities, CNG channels also exhibit some voltage sensitivity and are permeable to both monovalent and divalent cations, making it an ideal common precursor.[26] (c) More recently, Durell and Guy[29] showed that a Ca^{2+} channel with a 1D-6TM motif could be detected in the akylaphilic bacterium *Bacillus halodurans*\pard plain. This suggests that more mutations conferring Ca^{2+} selectivity in bacterial 1D-6TM channels occurred before any gene duplication occurred and prior to the development of lower eukaryotes (protozoans), where 4D-6TM Ca^{2+} channels have been identified.[26,29]

The first 4D-6TM proteins were voltage-dependent Ca^{2+} channels (VDCC), with early gene identification revealing multiple channels within the same tissue or cell. Eventually, Ca^{2+} channels were classified as low-voltage activated (LVA) or high-voltage activated (HVA) VDCC (see below and Catterall[30] for review). Ca^{2+} influx via VDCC has already been established as an effector or trigger in numerous cellular processes, with the different channel subtypes sometimes playing different roles. The variety of functional roles for VDCC correlates well with the significant structural diversity between the 10 VDCC α subunits currently identified ($\alpha_{1A\text{-}1I}$, α_{1S}).[30] Although the six isoforms identified in human PASMC represent each of the five Ca^{2+} channel subtypes, there is only electrophysiological evidence for the L- and T-type channels in PASMC[31,32] (also see below). As for voltage-gated K^+ channels, the associated genes are encoded on at least five human chromosomes, with no grouping of α–subunits encoding for similar currents on the same chromosome. For example, α_{1C} and α_{1D}, both encoding for L-type VDCC in human PASMC, are located on chromosomes 12 and 3, respectively, while those encoding for T-, N-, R- and P/Q-type channels are scattered on chromosomes 17, 9, 1 and 19, respectively [Figure 5]. Furthermore, while the structure of T-type VDCC is very similar to that of LVA channels, the sequence identity between them is <25%, implying that the HVA and LVA subfamilies represent radically different evolutionary branches.[26]

Like T-type Ca^{2+} currents ($I_{Ca(T)}$), Na^+ currents are rapidly activating transient currents activated at more negative membrane potentials. In lower eukaryotes, Ca^{2+} was the primary charge carrier;[26] purely Na^+-dependent action potentials were not common until the advent of the early metazoans. This has led to speculation that low-voltage activated and rapidly activating Na^+ channels evolved from Ca^{2+} channels in parallel with the evolution of the first nervous systems. Sequence analysis has shown that ligand-binding sites (e.g., carboxy-terminal calmodulin-binding site) may be conserved within the 4D-6TM voltage-gated Ca^{2+} and Na^+ channels, suggesting a similar evolutionary precursor.[33,34] Of particular interest is a putative calmodulin (CaM)-binding site located in the carboxy-terminal regions of both Na^+ and Ca^{2+} channels.[33,34] Cloning of the first LVA channels verified that voltage-dependent Na^+ channels did evolve from T-type VDCC.[35] Eleven known Na^+ channel α–subunit genes (SCN1A-11A) bearing strong biophysical and sequence (~75% sequence identity) similarities have been identified in the skeletal, cardiac and uterine muscles and in the human brain,[26,36,37] and bear approximately 75% sequence identity to each other.[26] Because the isoforms bear strong similarities, even when expressed in heterologous systems, voltage-gated Na^+ channels are not generally grouped into families like their Ca^{2+} and K^+ counterparts. The SCN5A and 6A isoforms expressed in PASMC are typically found in cardiac and uterine muscle. Unlike K^+ and Ca^{2+} channel α–subunit genes, all Na^+ channel

α–subunit genes map within four chromosomes (2, 3, 12 and 17) containing homeobox (HOX) gene clusters.[37] HOX genes have been predicted to have existed in ancestral chordates, suggesting that the initial expansion of Na^+ channels is associated with multiple chromosome duplications occurring after the divergence from invertebrate to pre-vertebrate chordates. The fact that many of the SCN genes are clustered on two chromosomes also suggests that intrachromosomal duplications also occurred over time.

Voltage-gated Na^+ Channels

In a variety of excitable cells, including smooth muscle cells, voltage-gated Na^+ channels are responsible for generating action potentials. Activation of the channels induces membrane depolarization and thus increases $[Ca^{2+}]_{cyt}$ by promoting Ca^{2+} influx through the sarcolemmal VDCC and the reverse mode Na^+/Ca^{2+} exchanger.[38,39] While the activation of Na^+ channels may underlie the spontaneous action potentials observed in cardiac and skeletal muscle myocytes,[40] removal of extracellular Ca^{2+} abolished spontaneous action potentials in PASMC [Figure 3b], suggesting that the electrical excitability of PASMC is induced by multiple ion channel functions. Furthermore, voltage-gated Na^+ channels may serve as a pathway for Ca^{2+} entry under physiological and pathophysiological conditions.[41,42]

Biophysical properties of voltage-gated Na^+ currents (I_{Na})—The inward $I_{Na(V)}$ observed in PASMC possesses similar biophysical and pharmacological characteristics to those previously identified in other human vascular smooth muscle cells:[39,43-46] sensitivity to tetrodotoxin (≤1 μM for total inhibition), -60 to -50 mV activation threshold, -15 to 10 mV peak amplitude potential, -70 to -65 mV half-inactivation voltage (τ_{inact} ≤4 ms) and -25 to -15 mV half-activation voltage (τ_{act} ~1 ms). In cultured human PASMC dialyzed with Cs^+-containing solution, a rapidly inactivating inward Na^+ current is observed in the absence of extracellular Ca^{2+} [Figure 6a]. As mentioned above, the current activates at potentials close to -60 mV and peaks at approximately +10 mV [Figure 6a]. These currents also inactivate rapidly, with the half-inactivation ($V_{0.5}$) occurring at approximately -65 mV and complete inactivation occurs at -20 mV [Figure 6b]. Equimolar replacement of external Na^+ with *N*-methyl-D-glucamine (NMDG) or extracellular application of 1 μM tetrodotoxin (TTX) is sufficient to abolish the currents [Figure 6c], suggesting that the currents in PASMC are carried by Na^+ influx through the TTX-sensitive, voltage-gated Na^+ channels similar to those described in neurons and cardiomyocytes.[40] The window currents determined by the overlap between the activation and inactivation curves are in the voltage range of -60 to -20 mV in human PASMC cultured in growth medium [Figure 6b, right panel]; these values are similar to those in other vascular smooth muscle cells, suggesting the participation of Na^+ currents in the regulation of resting E_m in human PASMC.

Voltage-gated Na^+ channel genes expressed in human PASMC—A complex of three glycoprotein subunits form functional Na^+ channels: a pore-forming α–subunit and two β-subunits that modulate channel gating and membrane expression [Figure 7a].[47] The α–subunit alone can form a functional channel and is composed of four domains, each containing six transmembrane segments (S1–S6) and a pore loop (P region). Each S4 segment is believed to act as a voltage sensor, while the S5-pore loop-S6 segments form the transmembrane pore itself. Using reverse transcriptase-polymerase chain reaction (RT-PCR), seven Na^+ channel-related gene transcripts (SCN1B, 2A, 2B, 4A, 8A, 9A and 11A) have been detected in PASMC [Figure 7b]. Transcripts for SCN5A and SCN6A have not yet been detected in PASMC. All of these isoforms are expressed in the brain [Figure 7b]. The combined functional and molecular identification of Na^+ currents and channels in human PASMC suggest that voltage-gated Na^+ channel activity and expression may relate to PASMC excitability, contractility, proliferation and differentiation.

Phenotypical change of voltage-gated Na^+ channel expression in freshly dissociated and cultured VSMC—Voltage-gated TTX-sensitive Na^+ currents ($I_{Na(V)}$) have been described in several types of human vascular smooth muscle cells cultured from the aorta[43,44] and coronary[39,46] and pulmonary[43,45] arteries. On only rare occasions have $I_{Na(V)}$ been recorded in freshly dissociated human vascular smooth muscle cells, although they are readily detected when the same cells are cultured.[46] Although it may be due to a technical problem (e.g., the rapid inactivation of the currents and the large size of most freshly dissociated smooth muscle cells to record $I_{Na(V)}$), the relative inability to detect $I_{Na(V)}$ in freshly dissociated, but not cultured, cells from the same vascular bed may bear some relation to cell dedifferentiation and proliferation.[46] More specifically, voltage-gated Na^+ channel expression and activity may be required to facilitate the transition from a "contractile" to "synthetic" or "proliferative" phenotype.[48,49] However, $I_{Na(V)}$ have been recorded in both freshly dispersed rabbit[24] and cultured human[45] PASMC. This raises the possibility that the development and expression of functional voltage-gated Na^+ channels in cultured cells acts as a trigger for cell differentiation and proliferation, possibly via enhanced $[Ca^{2+}]_{cyt}$, as discussed below.

Functional properties of voltage-gated Na^+ channels in human PASMC—Na^+ channels appear to play an important role in the regulation of $[Ca^{2+}]_{cyt}$ and sarcolemmal Ca^{2+} influx by different mechanisms. Firstly, in cardiac myocytes, enhanced TTX-sensitive $I_{Na(V)}$ causes a localized transient increase in $[Na^+]_{cyt}$, thereby activating reverse-mode Na^+/Ca^{2+} exchange and increasing $[Ca^{2+}]_{cyt}$ with the subsarcolemmal space between the plasma membrane and SR.[41] The Ca^{2+} newly introduced into the cytoplasm can then trigger further Ca^{2+} release from the SR (which ultimately will cause contraction and stimulate proliferation and migration) or replenish SR Ca^{2+} pools by Ca^{2+}-ATPase-mediated re-uptake.[42,50] Secondly, TTX-sensitive Na^+ channels are promiscuous, i.e. they can allow permeation of other cations (such as Ca^{2+}) under certain conditions (e.g., absence of extracellular Na^+, presence of tracing doses of steroids such as ouabain and digoxin).[42,51] Ca^{2+} influx through promiscuous Na^+ channels can contribute to local and global cardiac Ca^{2+} signaling, especially in heart failure patients treated with digoxin.[42] In addition to its modulating $[Ca^{2+}]_{cyt}$, the permeability of Na^+ channels to Ca^{2+} may also play a role in the contractile-to-proliferative cellular transition. Thirdly, voltage-gated Na^+ channels are essential in the generation of action potentials in many excitable cells, thereby regulating $[Ca^{2+}]_{cyt}$ based on evidence from expressed SCN5A channels,[33,53] we can speculate that Ca^{2+}/CaM-mediated regulation of voltage-gated Na^+ channels may play an important role in the coupling of human PASMC excitation and contraction.

VDCC

In excitable cells, the opening of VDCC is a critical mechanism responsible for muscle contraction induced by neuronal and humoral stimulation. There are at least five types of VDCC described in neurons and cardiomyocytes: L-type, T-type, P/Q-type, R-type and N-type.[54,55] These Ca^{2+} channels have been sorted based on their electrophysiological, pharmacological, kinetic and molecular properties. VDCC have also been separated into two groups based on their activation voltage. HVA VDCC include all but T-type channels, with the latter classified as LVA VDCC. HVA channels activate at membrane potentials between -50 mV and -20 mV, while LVA channels activate at more negative potentials approximating -70 mV. Typically, only currents generated by L- and T-type channels have been measured in cardiovascular tissues, while all current types have been recorded in neuronal tissues.[54]

Whole-cell VDCC currents (I_{Ca})—In human PASMC, a large, slowly inactivating inward Ca^{2+} current is observed when cells are held at -70 mV and depolarized to 0 mV

[Figure 8a]. The current activates close to -20 mV, with a maximal activation of approximately +15 mV. Removal of extracellular Ca^{2+} abolishes the currents, confirming that the currents are due to Ca^{2+} influx. Nifedipine, a dihydropyridine blocker of VDCC, is also able to significantly inhibit the currents. The currents present in PASMC are, therefore, mainly due to Ca^{2+} influx through dihydropyridine-sensitive L-type Ca^{2+} channels. Less frequently, and while being held at a very negative potential (-100 mV), depolarization to a test potential to -20 mV can elicit a rapidly activating transient inward Ca^{2+} current [Figure 8b and c]. This transient current activates and inactivates rapidly in comparison with the L-type current [Figure 8a], with a threshold potential for activation of approximately -36 mV at a holding potential of -90 mV. The biophysical properties of these currents are very similar to the T-type Ca^{2+} current observed in aortic[56] and renal artery[57] smooth muscle cells, rat PASMC[58] and cardiomyocytes.[59]

Endogenously expressed genes that encode VDCC in human PASMC—As for voltage-gated Na^+ channels, the pore-forming VDCC α_1-subunits (10 identified isoforms) are composed of four, six transmembrane segment domains [Figure 9a] that, when expressed alone, can create functional channels.[47] The pore-forming S5-loop-S6 segments and the voltage-sensing S4 segments are integral to the function of α_1-subunits. Three different regulatory subunits are also part of the greater Ca^{2+} channel complex.[54,60-62] β–subunits (four isoforms with their associated subtypes) play multiple roles in regulating channel membrane expression of α_1-subunits, current kinetics and biophysical properties. Extracellular $\alpha_2\delta$-subunits (two isoforms plus their subtypes) that are attached to the plasma membrane via a disulfide linkage can influence current amplitude and inactivation rates, and likely play a major role in stabilizing the incorporation of the Ca^{2+} channel complex into the plasma membrane. Finally, γ-subunits (six known isoforms) may modulate channel assembly and channel subtype-specific current kinetics, both effects being highly dependent on the nature of the co-expressed β– and $\alpha_2\delta$-subunits [Figure 9a]. At the RNA level, transcripts for six pore-forming α_1-subunits have been detected in human PASMC, encoding for all five VDCC types: α_{1A} (P/Q-type), α_{1B} (N-type), α_{1C} and α_{1D} (L-type), α_{1E} (R-type) and α_{1G} (T-type) [Figure 9b]. Additionally, a variety of regulatory subunit isoforms are also present, including $\alpha_2\delta_1$ [Figure 9c], $\beta_{1\text{-}4}$ [Figure 9d] and γ_6 [Figure 9e] in human PASMC. From the current molecular and electrophysiological evidence, it may be speculated that the α_{1C}-subunit may encode the L-type VDCC while the α_{1G} encodes for the T-type VDCC in human PASMC.

Voltage-gated K^+ Channels

Functionally, both voltage-gated (Kv) channels and Ca^{2+}-activated K^+ (Kca) channels (see below) are sensitive to voltage changes. In other words, these channels are activated by membrane depolarization and are deactivated by membrane hyperpolarization. A fundamental difference between Kv and Kca channels is their response to Ca^{2+}: in vascular smooth muscle cells, Kv channels are inhibited by cytoplasmic Ca^{2+}[21,63] and Kca channels are activated by cytosolic Ca^{2+}.[19,64] The existence of other types of K^+ channels, such as inward rectifier (K_{IR}), ATP-sensitive (K_{ATP}) and tandem-pore (K_T) channels, has also been demonstrated in vascular smooth muscle cells.[19,65,66] This review focuses only on the voltage-dependent channels; Kv and Kca channels.

Classification based on unitary conductance—Macroscopic currents of Kv ($I_{K(V)}$) and Kca ($I_{K(Ca)}$) channels can be readily dissociated based on their pharmacological properties and Ca^{2+}-dependence. Additionally, the single-channel conductance for each of these channels can also serve to distinguish them from each other. The traces shown in Figure 10 are representative cell-attached recordings from PASMC, where multiple channel subtype openings can be recorded from the same patch using identical Ca^{2+}-containing

perfusion solutions. As shown in Figure 10a, large amplitude K^+ currents (a) and several small amplitude currents (b–f) can be recorded in a cell-attached membrane patch. In addition to the various amplitudes of the recorded K^+ currents, the duration of the channel openings varies in human PASMC. Examples of long-lasting channel and "flickery" openings are shown in Figures 10b and c. In cell-attached patches of PASMC, multiple amplitudes of outward K^+ currents can be elicited by steadily holding the patch at different potentials. Representative openings for channels with seven different conductance levels are shown in Figure 11. The large amplitude current (225 pS and 189 pS) openings are likely generated by the activation of large-conductance Kca channels,[67] while the 33 pS, 81 pS and 6 pS channels may represent unitary currents through different Kv channels or small to intermediate conductance Kca channels.

In addition to its regulation of current amplitude, membrane potential can also affect the gating properties of these channels, e.g. the open probability (P_{open}). For the 189 pS channel shown in Figure 10, P_{open} increased with membrane depolarization from 0.0005 at 0 mV to 0.014 at +50 mV and 0.27 at +90 mV. Similarly P_{open} for the 33 pS channel increased from 0.04 at +60 mV to 0.43 at +90 mV, from 0.009 at +40 mV to 0.01 at +90 mV for the 141 pS channel and from 0.007 at +40 mV to 0.02 at +90 mV for the 6 pS channel. Therefore, both the single channel amplitude and the open probability of Kca and Kv channels are influenced by membrane potential in human PASMC.

Whole-cell voltage-gated K^+ (Kv) currents—In order to record optimal whole-cell (macroscopic) Kv currents ($I_{K(V)}$), cells are commonly perfused with Ca^{2+}-free bath solution (plus 1 mM EGTA) and dialyzed with Ca^{2+}-free pipette solution (plus 10 mM EGTA). Depolarizing the cells from a holding potential of -70 mV to a series of test potentials ranging from -60 mV to +80 mV elicits outward K^+ currents, with a threshold potential of activation at approximately -45 mV. Four families of whole-cell $I_{K(V)}$ currents can be distinguished based on their activation and inactivation kinetics: (i) rapidly activating and slowly inactivating $I_{K(V)}$ [Figure 12a], (ii) rapidly activating and non-inactivating $I_{K(V)}$ [Figure 12b], (iii) slowly activating and non-inactivating $I_{K(V)}$ [Figure 12c] and (iv) rapidly activating and rapidly inactivating $I_{K(V)}$ [Figure 12d]. Activation time constants (τ_{act}) can be separated into two components corresponding to the rapidly and slowly activating currents (<3 ms and >3 ms, respectively) [Figure 12e, top panel]. Inactivation constants (τ_{inact}) are much more variable, as shown in Figure 12e, bottom panel, with the midpoint between rapid and slow inactivation being approximately 100 ms. The half-activation occurs at +25 mV for each type of current. In PASMC, the family of Kv channels can thus be grossly divided into two categories: (a) delayed rectifier Kv channels generating slowly activating and non- or slowly inactivating currents and (b) rapidly activating and rapidly inactivating currents originating from the activation of transient "A"-type currents similar to those observed in phasic smooth muscle, cardiomyocytes and neurons.[68-71]

Extracellular application of 5 mM 4-AP, a common K_v channel inhibitor, reversibly decreases K_v currents [Figure 13]. While the slow inactivation kinetics of three of the different currents are typical of most native delayed-rectifier K^+ currents recorded in vascular SMCs,[19,25] the 4-AP-sensitive rapidly activating and inactivating current may represent a different class of K^+ current less commonly observed in vascular SMC. Based on its rapid inactivation (<100 ms) kinetics, this component closely resembles the transient I_A-type current that has been observed in phasic smooth muscle cells,[71,72] cardiac cells[68] and neurons.[70] Heteromeric assembly of K^+ channel α–subunits may account for the notable diversity of K^+ currents within the same cell system. When the electrophysiological properties of PASMC Kv currents are compared with those generated by cloned Kv channel α–subunits,[28,73-75] it is clear that the native channels' properties are intermediaries of those different clones forming the functional channels.

The behavior of single channels within a patch provides some evidence for the heteromeric assembly of the pore-forming units [Figure 10]. Cloned Kv channels have a wide range of single-channel conductances that do not always match with the conductance of native Kv channels. For example, the single-channel conductances for Kv1.1, Kv1.2 and Kv1.5 channels expressed in heterologous expression systems are reported to be 10 pS, 9–17 pS and 8 pS, respectively.[28,76,77] The conductance of native Kv channels in vascular SMC at physiological K^+ concentrations (5 mM internal, 140 mM external) ranges between 5 pS and 11 pS,[72,78] and between 15 pS and 70 pS in symmetrical (140 mM) K^+ conditions.[79-81] While the differences between native and cloned Kv conductances may relate to differences in the expression systems (e.g., pulmonary artery vs. HEK 293 cells), splicing or post-translational modifications, it is quite likely that native Kv channels are heterotetramers.

The association of multiple β–subunits with the functional α–tetramer may further influence the biophysical properties of native currents,[73] including those in human PASMC. Cytoplasmic Kv channel β–subunits associate with the S6 segment and carboxy-terminal region of Kvα–subunits via their own highly conserved carboxy terminus.[82] The most dramatic functional effect of Kv channel β-subunit association with Kv channel α is to confer inactivation onto the non-inactivating channels [Figure 14] and to confer redox and O_2 sensitivity onto the Kv channels.[83,84] In extreme cases, they convert non-inactivating Kv currents into rapidly inactivating transient currents.[85] In the case of the Kv channel β1-subunit, this occurs via the pore-blocking effect of an amino-terminal inactivation ball domain similar to that found on the “subunit.[85] Other β-subunits modulate current kinetics by shifting the activation curve, slowly deactivating the current, enhancing slow inactivation or altering peak current amplitude by acting as an open-channel blocker.[82,86] Finally, Kv channel β–subunits may participate in α–subunit assembly and transport to the plasma membrane, and enhance the interaction of α–subunits with protein kinases.[82,87] Given the diversity of roles and properties of Kv α– and β-subunits, it is not altogether surprising that Kv channel activity is central to numerous processes that rely on membrane potential regulation, such as hypoxic pulmonary vasoconstriction,[21,88-90] cell proliferation[6,91] and myogenic reactivity.[92]

Kv channel genes expressed in human PASMC—As mentioned above, native Kv channels are believed to be heteromeric tetramers composed of the pore-forming α–subunits and regulatory cytoplasmic β-subunits (α_4/β_4)[28,93] [Figure 15a]. Transcripts of Kv channel genes detected by RT-PCR on mRNA isolated from human PASMC and brain tissues are shown for each Kv channel subunit in Table 2. Brain tissue is commonly used as a positive control for the mRNA expression of ion channels due to its high expression of the majority of known ion channels. In human PASMC, at least 22 Kvα–subunits and 3 Kvβ-subunits [Figure 15b] have been identified. It is currently unknown as to how many of these transcripts are transcribed leading to expression of a functional channel/protein in PASMC. Figure 15c shows a phylogenetic diagram of Kv channels.

Macroscopic Ca^{2+}-activated K^+ currents—To record Kca currents, cells need to be superfused with 1.8 mM Ca^{2+}-containing bath solution and dialysed with an EGTA-free pipette solution. Depolarization from a holding potential of -70 mV to a series of test potentials ranging from -60 mV to +80 mV will elicit both Kca and Kv currents. The noisy currents dominant at positive potentials are representative of whole-cell Kca currents ($I_{K(Ca)}$) observed in freshly dissociated animal vascular smooth muscle cells.[21,69] In direct comparison with $I_{K(V)}$, $I_{K(Ca)}$ activate slowly with relatively little inactivation. Extracellular application of known inhibitors of Kca channels such as 1 mM TEA, 50 nM iberiotoxin or 50 nM charybdotoxin can significantly block the noisy $I_{K(Ca)}$ while having a negligible effect on $I_{K(V)}$. These findings in PASMC are consistent with observations in systemic vascular smooth muscle cells.[19,78,80] Dialysis of PASMC with a high (500 μM) Ca^{2+}

pipette solution (containing 8.8 mM EGTA and 10 mM $CaCl_2$) yields slowly activating outward currents that are significantly inhibited by extracellular application of the Kca channel blockers iberiotoxin and charybdotoxin. The slow activation kinetics of the $I_{K(Ca)}$ is consistent with the kinetics of the currents measured in cells transfected with the maxi-K^+ channel gene, hSlo-α_1.[94,95]

In cell-attached patches of PASMC, increased $[Ca^{2+}]_{cyt}$ by FCCP (which depolarizes and releases Ca^{2+} from mitochondria[96]) causes a significant increase in the steady-state open probability of the large-conductance $I_{K(Ca)}$ [Figure 16a]. Extracellular application of dihydroepiandrosterone, an agent that opens Kca channels via cAMP/cGMP-independent pathways,[97] also increases the P_{open} of large-conductance $I_{K(Ca)}$ [Figure 16b]. Cyclopiazonic acid causes Ca^{2+} mobilization from intracellular stores and, when applied in the cell-attached configuration, can increase P_{open} of a smaller-conductance $I_{K(Ca)}$ (47 pS) [Figure 16c] at +70 mV. It can therefore be inferred that two types of Kca channels, a large- and a small- or intermediate-conductance channel, are functionally expressed in human PASMC, and that they are synergistically regulated by membrane potential and $[Ca^{2+}]_{cyt}$.

Molecular identities of Kca channels in human PASMC—Unlike the mainly heterotetrameric Kv channels, Kca channels are predominantly homomeric tetramers composed of the pore-forming α–subunits and the auxiliary β-subunits [Figure 17a].[95] Several human Kca channel α–subunits that encode the large (maxi-Kca)- and small (SKca)-conductance Kca channels have been cloned and characterized in vascular SMC.[98,99] In addition to the pore-forming α–subunit, several β-subunits have also been identified.[99] Maxi-Kca α_1 (hSlo-α_1) is highly expressed in human PASMC [Figure 17a]. Four β-subunits (Maxi-Kca β1-4) are also detected by RT-PCR in PASMC [Figure 17b]. Three (SK2-4) pore-forming subunits are observed at the mRNA level for SKca channels [Figure 17c].

Table 3 shows the biophysical and pharmacological properties, along with the molecular identifies of, voltage-dependent cation channels in human PASMC. The information shown in Table 3 is certainly incomplete and it is important to conduct more studies to reveal all voltage-dependent cation channels that are functionally expressed in animal and human PASMC.

Contribution of Cation Channels to the Regulation of E_m and $[Ca^{2+}]_{cyt}$ in Human PASMC

As discussed, membrane potential is primarily determined by the concentration gradients across the plasma membrane of electrically charged ions, mainly Na^+, Ca^{2+}, K^+ and Cl^+, and their relative permeability. At rest, the concentration of intracellular K^+ (~140 mM) is much greater than that of the extracellular space (~5 mM) because of Na^+-K^+ ATPase pump activity, and the K^+ permeability across the plasma membrane is far greater than that of Na^+, Ca^{2+} and Cl^-.[15,106] Therefore, the resting E_m is mainly determined by the permeability of K^+ ($E_K \approx$ -85 mV) and the activity of Na^+-K^+ ATPase. Extracellular application of 5 mM 4-AP, which is known to reduce $I_{K(V)}$ [Figure 13], can reversibly cause membrane depolarization in human PASMC, whereas iberiotoxin, an inhibitor of Kca channels, has little effect on E_m. Increasing extracellular K^+ concentration (e.g., from 4.7 mM to 60 mM) also shifts the K^+ equilibrium potential and depolarizes E_m. It can, therefore, be proposed that 4-AP-sensitive Kv channels are active and contribute to the regulation of the resting E_m in PASMC.[25] E_m is an important determinant of $[Ca^{2+}]_{cyt}$ in SMC because of the voltage dependence of Ca^{2+} influx via voltage-dependent L-type VDCC[106,109] and the reverse mode of Na^+/Ca^{2+} exchanger.[110,111] Consistent with its inhibitory effect on Kv channels and depolarizing effect on PASMC membrane, extracellular application of 4-AP also reversibly increases $[Ca^{2+}]_{cyt}$ in PASMC and causes pulmonary vasoconstriction [Figure 18]. Membrane depolarization generated by raising the extracellular K^+ concentration from

4.7 mM to 60 mM results from an ~20 mV shift of E_K toward less-negative potentials. As a result of this rightward shift in E_K and the subsequent depolarization of E_m, $[Ca^{2+}]_{cyt}$ is elevated [Figure 18b], an effect significantly attenuated by the removal of extracellular Ca^{2+}. Membrane depolarization-mediated elevation of $[Ca^{2+}]_{cyt}$ is therefore mainly due to Ca^{2+} influx through nifedipine-sensitive VDCC in human PASMC.

Both excitable and quiescent cells possess a negative resting E_m. E_m is known to control electrical excitability (e.g., generation and propagation of action potentials), muscle contraction, apoptosis[112-114] and gene expression.[115,116] From the latter functions, it is apparent that the mechanisms controlling E_m and $[Ca^{2+}]_{cyt}$ are interrelated. Membrane depolarization elevates $[Ca^{2+}]_{cyt}$ mainly by activating VDCC[19,25,109,117,118] and the reverse-mode Na^+/Ca^{2+} exchanger[110,111,119] in the plasma membrane. In smooth muscle cells, the voltage window of sarcolemmal L-type voltage-gated Ca^{2+} channels for sustained elevation of $[Ca^{2+}]_{cyt}$ ranges from -40 mV to -20 mV, and peaks at -30 mV,[109] similar to what has been observed in human PASMC. The Na^+/Ca^{2+} exchanger has a reversal potential ($E_{Na\text{-}Ca}$) of approximately -47 mV at rest, based on the equation: $E_{Na\text{-}Ca}=3E_{Na}\text{-}2E_{Ca}$,[111] where E_{Na} is the Na^+ equilibrium potential (approximately +66 mV) and E_{Ca} is the Ca^{2+} equilibrium potential (approximately +122 mV). Membrane depolarization to potentials less negative than $E_{Na\text{-}Ca}$ would activate the reverse-mode Na^+/Ca^{2+} exchanger and promote Ca^{2+} influx.[110,111,119] Thus, the sustained membrane depolarization in PASMC may produce a constant Ca^{2+} influx through voltage-gated Ca^{2+} channels[106,109] and an inward Ca^{2+} transportation via the reverse mode of Na^+/Ca^{2+} exchange, and contribute to maintain the elevated $[Ca^{2+}]_{cyt}$ that is crucial for PASMC contraction and proliferation. As discussed earlier, Na^+ channel activation by membrane depolarization can also modulate $[Ca^{2+}]_{cyt}$ by (i) controlling $[Na^+]_{cyt}$, thereby modulating Na^+/Ca^{2+} exchange activity, (ii) non-selective permeation of Ca^{2+} ions through Na^+ channels and (iii) rapid Na^+-induced depolarization and subsequent VDCC activation.

While Na^+ and Ca^{2+} channel activation has a tendency to depolarize cells and enhance $[Ca^{2+}]_{cyt}$, K^+ channel activation hyperpolarizes the membrane and decreases sarcolemmal Ca^{2+} influx. Because of their voltage- and/or Ca^{2+}-dependence, K^+ channels are key elements in the maintenance of E_m to the “near-resting” level. This review reflects on data that an inhibition of Kv channels with 4-AP induces membrane depolarization and increases $[Ca^{2+}]_{cyt}$ by opening the nifedipine-sensitive L-type VDCC in human PASMC. An increase in $[Ca^{2+}]_{cyt}$ is believed to play an important role in stimulating cell growth by activating protein kinases and transcription factors that are essential for the progression of cell cycle.[115,116,120-122] Kv channels in PASMC may play an important role in modulating pulmonary vascular contractility and remodeling via regulating E_m and $[Ca^{2+}]_{cyt}$. Indeed, the roles of both Kca and Kv channels as feedback modulators of myogenic tone and agonist-induced vascular tone in systemic[123-125] and pulmonary arteries[63,126-132] are well documented.

Conclusions

In PASMC, EC-coupling is mainly achieved by a rise in $[Ca^{2+}]_{cyt}$, which is controlled by two related mechanisms, voltage-sensitive Ca^{2+} influx (electromechanical coupling) and ligand-mediated Ca^{2+} influx and mobilization (pharmacomechanical coupling). Membrane potential (E_m) and ion diffusion across the plasma membrane are dominantly regulated by the function and expression of ion-selective channels embedded in the plasma membrane. In addition, the activity of plasmalemmal ion channels and homeostasis of intracellular ions play important roles in the regulation of cell excitability, contraction, gene expression, proliferation, differentiation and apoptosis.[22,102,133] Electromechanical coupling mechanisms cause tonic and phasic vasomotor tone in blood vessels[106,134] and participate

in regulating cell proliferation[6] and protein/gene expression.[135] An understanding of the electrophysiological properties and molecular composition of voltage-dependent ion channels in human PASMC may provide important information for the development of effective therapeutic approaches for patients with pulmonary vascular diseases.

Pulmonary vasoconstriction and vascular remodeling (i.e., intimal and medial hypertrophy due to smooth muscle cell proliferation and migration) greatly contribute to the elevated pulmonary vascular resistance in patients with pulmonary hypertension.[136,137] Because both E_m and Ca^{2+} are recognized as important modulators of both vascular tone and cell growth, it is plausible that ion channels also play a role in these processes, particularly those ion channels that regulate and can be regulated by E_m and Ca^{2+}. Dysfunctional K^+ channels have been demonstrated to be involved in the pathogenesis of idiopathic pulmonary arterial hypertension.[8,9] There is no direct evidence to suggest alterations in Na^+ channel gene expression or function in pulmonary hypertension-induced vascular remodeling. Nonetheless, Na^+ channel-mediated regulation of $[Ca^{2+}]_{cyt}$ may be important in the modulation of cell proliferation. Similarly, VDCC upregulation or “gain-in-function” has not been directly involved in the pathogenesis of pulmonary arterial hypertension, although any abnormalities in its expression or function may alter the remodeling process. However, recent observations have reported an increase in store-operated Ca^{2+} channel activity during human PASMC proliferation,[138] suggesting that alternative Ca^{2+} influx pathways may be involved in the pulmonary vascular remodeling process. Targeting Ca^{2+} - (and Na^+-) permeable channels in the plasma membrane of pulmonary vascular smooth muscle cells and myofibroblasts is an efficient approach to develop a novel therapy for patients with pulmonary arterial hypertension.

Acknowledgments

This work was supported by grants from the National Heart, Lung and Blood Institute of the National Institutes of Health (HL 066012 and HL 098053). We would like to thank Mehran Mandegar, Jian Wang, Tiffany Sison and Elyssa D. Burg for their excellent work for generating the unpublished data shown in this review.

References

1. Casteels R, Kitamura K, Kuriyama H, Suzuki H. Excitation-contraction coupling in the smooth muscle cells of the rabbit main pulmonary artery. J Physiol. 1977; 271:63–79. [PubMed: 915834]
2. Madden JA, Dawson CA, Harder DR. Hypoxia-induced activation in small isolated pulmonary arteries from the cat. J Appl Physiol. 1985; 59:113–9. [PubMed: 4030552]
3. Beech DJ. Actions of neurotransmit ers and other messengers on Ca^{2+} channels and K^+ channels in smooth muscle cells. Pharmacol Ther. 1997; 73:91–119. [PubMed: 9131720]
4. Wang Q, Large WA. Action of histamine on single smooth muscle cells dispersed from the rabbit pulmonary artery. J Physiol. 1993; 468:125–39. [PubMed: 8254503]
5. Devine CE, Somlyo AV, Somlyo AP. Sarcoplasmic reticulum and excitation-contraction coupling in mammalian smooth muscles. J Cell Biol. 1972; 52:690–718. [PubMed: 5061887]
6. Platoshyn O, Golovina VA, Bailey CL, Limsuwan A, Krick S, Juhaszova M, et al. Sustained membrane depolarization and pulmonary artery smooth muscle cell proliferation. Am J Physiol Cell Physiol. 2000; 279:C1540–9. [PubMed: 11029301]
7. Pauly RR, Bilato C, Sollot SJ, Monticone R, Kelly PT, Lakat a EG, et al. Role of calcium/calmodulin-dependent protein kinase II in the regulation of vascular smooth muscle cell migration. Circulation. 1995; 91:1107–15. [PubMed: 7850948]
8. Yuan JX, Aldinger AM, Juhaszova M, Wang J, Conte JV Jr, Gaine SP, et al. Dysfunctional voltage-gated K^+ channels in pulmonary artery smooth muscle cells of patients with primary pulmonary hypertension. Circulation. 1998; 98:1400–6. [PubMed: 9760294]
9. Yuan XJ, Wang J, Juhaszova M, Gaine SP, Rubin LJ. Attenuated K^+ channel gene transcription in primary pulmonary hypertension. Lancet. 1998; 351:726–7. [PubMed: 9504523]

10. Cox RH, Folander K, Swanson R. Differential expression of voltage-gated K^+ channel genes in arteries from spontaneously hypertensive and Wistar-Kyoto rats. Hypertension. 2001; 37:1315–22. [PubMed: 11358947]
11. Liu Y, Hudetz AG, Knaus HG, Rusch NJ. Increased expression of Ca^{2+}-sensitive K^+ channels in the cerebral microcirculation of genetically hypertensive rats. Evidence for their protection against cerebral vasospasm. Circ Res. 1998; 82:729–37. [PubMed: 9546382]
12. Martens JR, Gelband CH. Alterations in rat interlobar artery membrane potential and K^+ channels in genetic and nongenetic hypertension. Circ Res. 1996; 79:295–301. [PubMed: 8756007]
13. Martens JR, Gelband CH. Ion channels in vascular smooth muscle: Alterations in essential hypertension. Proc Soc Exp Biol Med. 1998; 218:192–203. [PubMed: 9648936]
14. Beuckelmann DJ, Näbauer M, Erdmann E. Alterations of K^+ currents in isolated human ventricular myocytes from patients with terminal heart failure. Circ Res. 1993; 73:379–85. [PubMed: 8330380]
15. Jones, AW. Content and fluxes of electrolytes. In: Bohr, DF.; Somlyo, AP.; Sparks, HV., editors. Handbook of Physiology, The Cardiovascular System Vascular Smooth Muscle. Baltimore, MD: Williams and Wilkins; 1980. p. 253-99.
16. Hamill OP, Marty A, Neher E, Sakmann B, Sigworth FJ. Improved patch-clamp techniques for high-resolution current recording from cells and cell-free membrane patches. Pflugers Arch. 1981; 391:85–100. [PubMed: 6270629]
17. Hille, B. Ionic channels of excitable membranes. 2nd. Sunderland, Massachusetts: Sinauer Associates Inc.; 1992.
18. Toro L, Gonzalez-Robles A, Stefani E. Electrical properties and morphology of single vascular smooth muscle cells in culture. Am J Physiol. 1986; 251:C763–73. [PubMed: 2430464]
19. Nelson MT, Quayle JM. Physiological roles and properties of potassium channels in arterial smooth muscle. Am J Physiol. 1995; 268:C799–822. [PubMed: 7733230]
20. Post JM, Hume JR, Archer SL, Weir EK. Direct role for potassium channel inhibition in hypoxic pulmonary vasoconstriction. Am J Physiol. 1992; 262:C882–90. [PubMed: 1566816]
21. Post JM, Gelband CH, Hume JR. $[Ca^{2+}]_i$ inhibition of K^+ channels in canine pulmonary artery. Novel mechanism for hypoxia-induced membrane depolarization. Circ Res. 1995; 77:131–9. [PubMed: 7788871]
22. Somlyo AP, Somlyo AV. Smooth muscle: Excitation-contraction coupling, contractile regulation, and the cross-bridge cycle. Alcohol Clin Exp Res. 1994; 18:138–43. [PubMed: 8198210]
23. Kuriyama H, Suzuki H. Electrical property and chemical sensitivity of vascular smooth muscles in normotensive and spontaneously hypertensive rats. J Physiol. 1978; 285:409–24. [PubMed: 745102]
24. Okabe K, Kitamura K, Kuriyama H. The existence of a highly tetrodotoxin sensitive Na channel in freshly dispersed smooth muscle cells of the rabbit main pulmonary artery. Pflugers Arch. 1988; 411:423–8. [PubMed: 2456516]
25. Yuan XJ. Voltage-gated K^+ currents regulate resting membrane potential and $[Ca^{2+}]_i$ in pulmonary arterial myocytes. Circ Res. 1995; 77:370–8. [PubMed: 7542182]
26. Anderson PA, Greenberg RM. Phylogeny of ion channels: Clues to structure and function. Comp Biochem Physiol B Biochem Mol Biol. 2001; 129:17–28. [PubMed: 11337248]
27. Strong M, Chandy KG, Gutman GA. Molecular evolution of voltage-sensitive ion channel genes: On the origns of electrical excitability. Mol Biol Evol. 1993; 10:221–42. [PubMed: 7680747]
28. Coetzee WA, Amarillo Y, Chiu J, Chow A, Lau D, McCormack T, et al. Molecular diversity of K^+ channels. Ann N Y Acad Sci. 1999; 868:233–85. [PubMed: 10414301]
29. Durell SR, Guy HR. A putative prokaryote voltage-gated Ca^{2+} channel with only one 6TM motif per subunit. Biochem Biophys Res Comm. 2001; 281:741–6. [PubMed: 11237720]
30. Catterall WA. From ionic currents to molecular mechanisms: The structure and function of voltage-gated sodium channels. Neuron. 2000; 26:13–25. [PubMed: 10798388]
31. Shimoda LA, Sham JS, Shimoda TH, Sylvester JT. L-type Ca^{2+} channels, resting $[Ca^{2+}]_i$, and ET-1-induced responses in chronically hypoxic pulmonary myocytes. Am J Physiol Lung Cell Mol Physiol. 2000; 279:L884–94. [PubMed: 11053024]

32. Zhou C, Wu S. T-type calcium channels in pulmonary vascular endothelium. Microcirculation. 2006; 13:645–56. [PubMed: 17085425]
33. Mori M, Konno T, Ozawa T, Murata M, Imoto K, Nagayama K. Novel interaction of the voltage-dependent sodium channel (VDSC) with calmodulin: Does VDSC acquire calmoduln-mediated Ca^{2+} sensitivity? Biochemistry. 2000; 39:1316–23. [PubMed: 10684611]
34. Zühlke RD, Pitt GS, Deisseroth K, Tsien RW, Reuter H. Calmodulin supports both inactivation and facilitation of L-type calcium channels. Nature. 1999; 399:159–62. [PubMed: 10335846]
35. Spafford JD, Spencer AN, Gallin WJ. Genomic organization of a voltage-gated Na^+ channel in a hydrozoan jellyfish: Insights into the evolution of voltage-gated Na^+ channel genes. Receptors Channels. 1999; 6:493–506. [PubMed: 10635065]
36. Goldin AL. Resurgence of sodium channel research. Annu Rev Physiol. 2001; 63:871–94. [PubMed: 11181979]
37. Plummer NW, Meisler MH. Evolution and diversity of mammalian sodium channel genes. Genomics. 1999; 57:323–31. [PubMed: 10198179]
38. Arnon A, Hamlyn JM, Blaustein MP. Na^+ entry via store-operated channels modulates Ca^{2+} signaling in arterial myocytes. Am J Physiol Cell Physiol. 2000; 278:C163–73. [PubMed: 10644524]
39. Boccara G, Choby C, Frapier JM, Quignard JF, Nargeot J, Dayanithi G, et al. Regulation of Ca^{2+} homeostasis by atypical Na^+ currents in cultured human coronary myocytes. Circ Res. 1999; 85:606–13. [PubMed: 10506485]
40. Fozzard HA, January CT, Makielski JC. New studies of the excitatory sodium currents in heart muscle. Circ Res. 1985; 56:475–85. [PubMed: 2579746]
41. Leblanc N, Hume JR. Sodium current induced release of calcium from cardiac sarcoplasmic reticulum. Science. 1990; 248:372–6. [PubMed: 2158146]
42. Santana LF, Gómez AM, Lederer WJ. Ca^{2+} flux through promiscuous cardiac Na^+ channels: Slip-mode conductance. Science. 1998; 279:1027–33. [PubMed: 9461434]
43. Choby C, Mangoni ME, Boccara G, Nargeot J, Richard S. Evidence for tetrodotoxin-sensitive sodium currents in primary cultured myocytes from human, pig and rabbit arteries. Pflugers Arch. 2000; 440:149–52. [PubMed: 10864008]
44. Cox RH, Zhou Z, Tulenko TN. Voltage-gated sodium channels in human aortic smooth muscle cells. J Vasc Res. 1998; 35:310–7. [PubMed: 9789111]
45. James AF, Okada T, Horie M. A fast transient outward current in cultured cells from human pulmonary artery smooth muscle. Am J Physiol. 1995; 268:H2358–65. [PubMed: 7611488]
46. Quignard JF, Ryckwaert F, Albat B, Nargeot J, Richard S. A novel tetrodotoxin-sensitive Na^+ current in cultured human coronary myocytes. Circ Res. 1997; 80:377–82. [PubMed: 9048658]
47. Felix R. Channelopathies: Ion channel defects linked to heritable clinical disorders. J Med Genet. 2000; 37:729–40. [PubMed: 11015449]
48. Li S, Sims S, Jiao Y, Chow LH, Pickering JG. Evidence from a novel human cell clone that adult vascular smooth muscle cells can convert reversibly between noncontractile and contractile phenotypes. Circ Res. 1999; 85:338–48. [PubMed: 10455062]
49. Sashihara S, Tshuji S, Matsui T. Oncogenes and signal transduction pathways involved in the regulation of Na^+ channel expression. Crit Rev Oncog. 1998; 9:19–34. [PubMed: 9754445]
50. Aggarwal R, Shorofsky SR, Goldman L, Balke CW. Tetrodotoxin-blockable calcium currents in rat ventricular myocytes: A third type of cardiac cell sodium current. J Physiol. 1997; 505:353–69. [PubMed: 9423179]
51. Cole WC, Chartier D, Martin M, Leblanc N. Ca^{2+} permeation through Na^+ channels in guinea pig ventricular myocytes. Am J Physiol. 1997; 273:H128–37. [PubMed: 9249483]
52. Deschenes I, Neyroud N, DiSilvestre D, Marban E, Yue DT, Tomaselli GF. Isoform-specifi c modulation of voltage-gated Na(+) channels by calmodulin. Circ Res. 2002; 90:E49–57. [PubMed: 11884381]
53. Tan HL, Kupershmidt S, Zhang R, Stepanovic S, Roden DM, Wilde AA, et al. A calcium sensor in the sodium channel modulates cardiac excitability. Nature. 2002; 415:442–7. [PubMed: 11807557]

54. Cat erall WA. Structure and regulation of voltage-gated Ca^{2+} channels. Annu Rev Cell Dev Biol. 2000; 16:521–55. [PubMed: 11031246]
55. Randall AD. The molecular basis of voltage-gated Ca^{2+} channel diversity: Is it time for T? J Membr Biol. 1998; 161:207–13. [PubMed: 9493126]
56. Sturek M, Hermsmeyer K. Calcium and sodium channels in spontaneously contracting vascular muscle cells. Science. 1986; 233:475–8. [PubMed: 2425434]
57. Hansen PB, Jensen BL, Andreasen D, Skøt O. Diff erential expression of T- and L-type voltage dependent calcium channels in renal resistance vessels. Circ Res. 2001; 89:630–8. [PubMed: 11577029]
58. Muramatsu M, Tyler RC, Rodman DM, McMurtry IF. Possible role of T-type Ca^{2+} channels in L-NNA vasoconstriction of hypertensive rat lungs. Am J Physiol. 1997; 272:H2612–21.
59. Balke CW, Rose WC, Marban E, Wier WG. Macroscopic and unitary properties of physiological ion flux through T-type Ca^{2+} channels in guinea-pig heart cells. J Physiol. 1992; 456:247–65. [PubMed: 1338097]
60. Restituito S, Cens T, Rousset M, Charnet P. Ca^{2+} channel inactivation heterogeneity reveals physiological unbinding of auxiliary b subunits. Biophys J. 2001; 81:89–96. [PubMed: 11423397]
61. Varadi G, Mori Y, Mikala G, Schwartz A. Molecular determinants of Ca^{2+} channel function and drug action. Trends Pharmacol Sci. 1995; 16:43–9. [PubMed: 7762082]
62. Walker D, De Waard M. Subunit interaction sites in voltage-dependent Ca^{2+} channels: Role in channel function. Trends Neurosci. 1998; 21:148–54. [PubMed: 9554724]
63. Gelband CH, Gelband H. Ca^{2+} release from intracellular stores is an initial step in hypoxic pulmonary vasoconstriction of rat pulmonary artery resistance vessels. Circulation. 1997; 96:3647–54. [PubMed: 9396467]
64. Peng W, Hoidal JR, Karwande SV, Farrukh IS. Effect of chronic hypoxia on K^+ channels: Regulation in human pulmonary vascular smooth muscle cells. Am J Physiol. 1997; 272:C1271–8. [PubMed: 9142852]
65. Koh SD, Monaghan K, Sergeant GP, Ro S, Walker RL, Sanders KM, et al. TREK-1 regulation by nitric oxide and cGMP-dependent protein kinase. An essential role in smooth muscle inhibitory neurotransmission. J Biol Chem. 2001; 276:44338–46. [PubMed: 11560940]
66. Mandegar M, Yu Y, Platoshyn O, Lapp BR, Rubin LJ, Yuan JX. Expression and function of tandem-pore K^+ channels in human pulmonary artery smooth muscle cells. Am J Respir Crit Care Med. 2002; 195:B53.
67. Peng W, Karwande SV, Hoidal JR, Farrukh IS. Potassium currents in cultured human pulmonary arterial smooth muscle cells. J Appl Physiol. 1996; 80:1187–96. [PubMed: 8926245]
68. Barry DM, Nerbonne JM. Myocardial potassium channels: Electrophysiological and molecular diversity. Annu Rev Physiol. 1994; 58:363–94. [PubMed: 8815800]
69. Beech DJ, Bolton TB. Two components of potassium current activated by depolarization of single smooth muscle cells from the rabbit portal vein. J Physiol. 1989; 418:293–309. [PubMed: 2621620]
70. Rogawski MA. The A-current: How ubiquitous a feature of excitable cells is it? Trends Neurosci. 1985; 8:214–9.
71. Vogalis F, Lang RJ. Identification of single transiently opening ('A-type') K channels in guinea-pig colonic myocytes. Pflugers Arch. 1994; 429:160–4. [PubMed: 7892100]
72. Beech DJ, Bolton TB. A voltage-dependent outward current with fast kinetics in single smooth muscle cells isolated from rabbit portal vein. J Physiol. 1989; 412:397–414. [PubMed: 2600838]
73. Coppock EA, Tamkun MM. Differential expression of Kv channel a- and b-subunits in the bovine pulmonary arterial circulation. Am J Physiol Lung Cell Mol Physiol. 2001; 281:L1350–60. [PubMed: 11704530]
74. Hulme JT, Coppock EA, Felipe A, Martens JR, Tamkun MM. Oxygen sensitivity of cloned voltage-gated K^+ channels expressed in the pulmonary vasculature. Circ Res. 1999; 85:489–97. [PubMed: 10488051]
75. Patel AJ, Honoré E. Molecular physiology of oxygen-sensitive potassium channels. Eur Respir J. 2001; 18:221–7. [PubMed: 11510795]

76. Clément-Chomienne O, Ishii K, Walsh MP, Cole WC. Identification, cloning and expression of rabbit vascular smooth muscle $K_V1.5$ and comparison with native delayed rectifier K^+ current. J Physiol. 1999; 515:653–67. [PubMed: 10066895]
77. Hart PJ, Overturf KE, Russell SN, Carl A, Hume JR, Sanders KM, et al. Cloning and expression of a Kv1.2 class delayed rectifier K^+ channel from canine colonic smooth muscle. Proc Natl Acad Sci U S A. 1993; 90:9659–63. [PubMed: 8415758]
78. Volk KA, Matsuda JJ, Shibata EF. A voltage-dependent potassium current in rabbit coronary artery smooth muscle cells. J Physiol. 1991; 439:751–68. [PubMed: 1910087]
79. Aiello EA, Malcolm AT, Walsh MP, Cole WC. b-Adrenoceptor activation and PKA regulate delayed rectifier K^+ channels of vascular smooth muscle cells. Am J Physiol. 1998; 275:H448–59. [PubMed: 9683432]
80. Gelband CH, Hume JR. Ionic currents in single smooth muscle cells of the canine renal artery. Circ Res. 1992; 71:745–58. [PubMed: 1381293]
81. Ishikawa T, Hume JR, Keef KD. Modulation of K^+ and Ca^{2+} channels by histamine H_1-receptor stimulation in rabbit coronary artery cells. J Physiol. 1993; 468:379–400. [PubMed: 7504729]
82. Martens JR, Kwak YG, Tamkun MM. Modulation of Kv channel a/b subunit interactions. Trends Cardiovasc Med. 1999; 9:253–8. [PubMed: 11094335]
83. Gulbis JM, Mann S, MacKinnon R. Structure of a voltage-dependent K+ channel beta subunit. Cell. 1999; 97:943–52. [PubMed: 10399921]
84. Pérez-García MT, López-López JR, González C. Kvb1.2 subunit coexpression in HEK293 cells confers O_2 sensitivity to Kv4.2 but not to Shaker channels. J Gen Physiol. 1999; 113:897–907. [PubMed: 10352037]
85. Rettig J, Heinemann SH, Wunder F, Lorra C, Parcej DN, Dolly JO, et al. Inactivation properties of voltage-gated K^+ channels altered by presence of b-subunit. Nature. 1994; 369:289–94. [PubMed: 8183366]
86. Rasmusson RL, Wang S, Castellino RC, Morales MJ, Strauss HC. The b subunit, Kvb1.2, acts as a rapid open channel blocker of NH_2 terminal deleted Kv1.4 a-subunits. Adv Exp Med Biol. 1997; 430:29–37. [PubMed: 9330716]
87. Gong J, Xu J, Bezanilla M, van Huizen R, Derin R, Li M. Diff erential stimulation of PKC phosphorylation of potassium channels by ZIP1 and ZIP2. Science. 1999; 285:1565–9. [PubMed: 10477520]
88. Park MK, Bae YM, Lee SH, Ho WK, Earm YE. Modulation of voltage-dependent K^+ channel by redox potential in pulmonary and ear arterial smooth muscle cells of the rabbit. Pflugers Arch. 1997; 434:764–71. [PubMed: 9306010]
89. Smirnov SV, Robertson TP, Ward JP, Aaronson PI. Chronic hypoxia is associated with reduced delayed rectifier K^+ current in rat pulmonary artery muscle cells. Am J Physiol. 1994; 266:H365–70. [PubMed: 8304521]
90. Yuan XJ, Goldman WF, Tod ML, Rubin LJ, Blaustein MP. Hypoxia reduces potassium currents in cultured rat pulmonary but not mesenteric arterial myocytes. Am J Physiol. 1993; 264:L116–23. [PubMed: 8447425]
91. Yu Y, Platoshyn O, Zhang J, Krick S, Zhao Y, Rubin LJ, et al. c-Jun decreases voltage-gated K^+ channel activity in pulmonary artery smooth muscle cells. Circulation. 2001; 104:1557–63. [PubMed: 11571252]
92. Knot HJ, Nelson MT. Regulation of membrane potential and diameter by voltage-dependent K^+ channels in rabbit myogenic cerebral arteries. Am J Physiol. 1995; 269:H348–55. [PubMed: 7631867]
93. Chandy, KG.; Gutman, GA. Voltage-gated K^+ channels. In: North, RA., editor. Ligand- and Voltage-Gated Ion Channels. Boca Raton, FL: CRC; 1995. p. 1-71.
94. Alioua A, Tanaka Y, Wallner M, Hofmann F, Ruth P, Meera P, et al. The large-conductance, voltage-dependent, and calcium-sensitive K^+ channel, Hslo, is a target of cGMP-dependent protein kinase phosphorylation *in vivo*. J Biol Chem. 1998; 273:32950–6. [PubMed: 9830046]
95. Toro L, Wallner M, Meera P, Tanaka Y. Maxi-Kca, a unique member of the voltage-gated K channel superfamily. News Physiol Sci. 1998; 13:112–7. [PubMed: 11390773]

96. Krick S, Platoshyn O, McDaniel SS, Rubin LJ, Yuan JX. Augmented K^+ currents and mitochondrial membrane depolarization in pulmonary artery myocyte apoptosis. Am J Physiol Lung Cell Mol Physiol. 2001; 281:L887–94. [PubMed: 11557592]

97. Farrukh IS, Peng W, Orlinska U, Hoidal JR. Effect of dehydroepiandrosterone on hypoxic pulmonary vasoconstriction: A Ca^{2+}-activated K^+-channel opener. Am J Physiol. 1998; 274:L186–95. [PubMed: 9486202]

98. Neylon CB, Lang RJ, Fu Y, Bobik A, Reinhart PH. Molecular cloning and characterization of the intermediate-conductance Ca^{2+}-activated K^+ channel in vascular smooth muscle: Relationship between Kca channel diversity and smooth muscle cell function. Circ Res. 1999; 85:e33–43. [PubMed: 10532960]

99. Tanaka Y, Meera P, Song M, Knaus HG, Toro L. Molecular constituents of maxi Kca channels in human coronary smooth muscle: Predominant a + b subunit complexes. J Physiol. 1997; 502:545–57. [PubMed: 9279807]

100. Stull JT, Kamm KE, Taylor DA. Calcium control of smooth muscle contractility. Am J Med Sci. 1988; 296:241–5. [PubMed: 2973750]

101. Berridge MJ. Calcium signalling and cell proliferation. Bioessays. 1995; 17:491–500. [PubMed: 7575490]

102. Means AR. Calcium calmodulin and cell cycle regulation. FEBS Lett. 1994; 347:1–4. [PubMed: 8013652]

103. Dolmetsch RE, Lewis RS, Goodnow CC, Healy JI. Differential activation of transcription factors induced by Ca^{2+} response amplitude and duration. Nature. 1997; 386:855–8. [PubMed: 9126747]

104. Ginty DD. Calcium regulation of gene expression: Isn't that spatial? Neuron. 1997; 18:183–6. [PubMed: 9052789]

105. Johnson CM, Hill CS, Chawla S, Treisman R, Bading H. Calcium controls gene expression via three distinct pathways that can function independently of the Ras/mitogen-activated protein kinases (ERKs) signaling cascade. J Neurosci. 1997; 17:6189–202. [PubMed: 9236230]

106. Nelson MT, Patlak JB, Worley JF, Standen NB. Calcium channels, potassium channels, and voltage dependence of arterial smooth muscle tone. Am J Physiol. 1990; 259:C3–18. [PubMed: 2164782]

107. Short AD, Bian J, Ghosh TK, Waldron RT, Rybak SL, Gill DL. Intracellular Ca^{2+} pool content is linked to control of cell growth. Proc Natl Acad Sci U S A. 1993; 90:4986–90. [PubMed: 8389460]

108. He H, Lam M, McCormick TS, Distelhorst CW. Maintenance of calcium homeostasis in the endoplasmic reticulum by Bcl-2. J Cell Biol. 1997; 138:1219–28. [PubMed: 9298978]

109. Fleischmann BK, Murray RK, Kotlikoff MI. Voltage window for sustained elevation of cytosolic calcium in smooth muscle cells. Proc Natl Acad Sci U S A. 1994; 91:11914–8. [PubMed: 7527547]

110. Kohomoto O, Levi AJ, Bridge JH. Relation between reverse sodium-calcium exchange and sarcoplasmic reticulum calcium release in guinea pig ventricular cells. Circ Res. 1994; 74:550–4. [PubMed: 8118963]

111. Blaustein MP, Lederer WJ. Sodium/calcium exchange: Its physiological implications. Physiol Rev. 1999; 79:763–854. [PubMed: 10390518]

112. Franklin JL, Sanz-Rodriguez C, Juhasz A, Deckwerth TL, Johnson EM Jr. Chronic depolarization prevents programmed death of sympathetic neurons *in vitro* but does not support growth: Requirement for Ca^{2+} influx but not Trk activation. J Neurosci. 1995; 15:643–64. [PubMed: 7823169]

113. Koike T, Martin DP, Johnson EM Jr. Role of Ca^{2+} channels in the ability of membrane depolarization to prevent neuronal death induced by trophic-factor deprivation: Evidence that levels of internal Ca^{2+} determine nerve growth factor dependence of sympathetic ganglion cells. Proc Natl Acad Sci U S A. 1989; 86:6421–5. [PubMed: 2548215]

114. Yu SP, Yeh CH, Sensi SL, Gwag BJ, Canzoniero LM, Farhangrazi ZS, et al. Mediation of neuronal apoptosis by enhancement of outward potassium current. Science. 1997; 278:114–7. [PubMed: 9311914]

115. Rosen LB, Ginty DD, Weber MJ, Greenberg ME. Membrane depolarization and calcium infl ux stimulate MEK and MAP kinase via activation of Ras. Neuron. 1994; 12:1207–21. [PubMed: 8011335]
116. Sheng M, McFadden G, Greenberg ME. Membrane depolarization and calcium induce c-fos transcription via phosphorylation of transcription factor CREB. Neuron. 1990; 4:571–82. [PubMed: 2157471]
117. Tsien RW, Tsien RY. Calcium channels, stores, and oscillations. Annu Rev Cell Biol. 1990; 6:715–60. [PubMed: 2177344]
118. Van Breemen C, Saida K. Cellular mechanisms regulating $[Ca^{2+}]_i$ smooth muscle. Annu Rev Physiol. 1989; 51:315–29. [PubMed: 2653185]
119. Sham JS, Cleemann L, Morad M. Gating of the cardiac Ca^{2+} release channel: The role of Na^+ current and Na^+-Ca^{2+} exchange. Science. 1992; 255:850–3. [PubMed: 1311127]
120. Chao TS, Byron KL, Lee KM, Villereal M, Rosner MR. Activation of MAP kinases by calcium-dependent and calcium-independent pathways.Stimulation by thapsigargin and epidermal growth factor. J Biol Chem. 1992; 267:19876–83. [PubMed: 1328184]
121. Dynlacht BD. Regulation of transcription by proteins that control the cell cycle. Nature. 1997; 389:149–52. [PubMed: 9296491]
122. Husain M, Jiang L, See V, Bein K, Simons M, Alper SL, et al. Regulation of vascular smooth muscle cell proliferation by plasma membrane Ca($^{2+}$)-ATPase. Am J Physiol. 1997; 272:C1947–59. [PubMed: 9227424]
123. Brayden JE, Nelson MT. Regulation of arterial tone by activation of calcium-dependent potassium channels. Science. 1992; 256:532–5. [PubMed: 1373909]
124. Jaggar JH, Mawe GM, Nelson MT. Voltage-dependent K^+ currents in smooth muscle cells from mouse gallbladder. Am J Physiol. 1998; 274:G687–93. [PubMed: 9575850]
125. Khan SA, Mathews WR, Meisheri KD. Role of calcium-activated K^+ channels in vasodilation induced by nitroglycerine, acetylcholine and nitric oxide. J Pharmacol Exp Ther. 1993; 267:1327–35. [PubMed: 7505330]
126. Barman SA. Pulmonary vasoreactivity to endothelin-1 at elevated vascular tone is modulated by potassium channels. J Appl Physiol. 1996; 80:91–8. [PubMed: 8847337]
127. Barman SA. Potassium channels modulate canine pulmonary vasoreactivity to protein kinase C activation. Am J Physiol. 1999; 277:L558–65. [PubMed: 10484463]
128. Hasunuma K, Rodman DM, McMurtry IF. Effects of K^+ channel blockers on vascular tone in the perfused rat lung. Am Rev Respir Dis. 1991; 144:884–7. [PubMed: 1928966]
129. Peng W, Hoidal JR, Farrukh IS. Regulation of Ca^{2+}-activated K^+ channels in pulmonary vascular smooth muscle cells: Role of nitric oxide. J Appl Physiol. 1996; 81:1264–72. [PubMed: 8889762]
130. Shimoda LA, Sylvester JT, Sham JS. Inhibition of voltage-gated K^+ current in rat intrapulmonary arterial myocytes by endothelin-1. Am J Physiol. 1998; 274:L842–53. [PubMed: 9612301]
131. Yuan XJ, Sugiyama T, Goldman WF, Rubin LJ, Blaustein MP. A mitochondrial uncoupler increases Kca currents but decreases Kv currents in pulmonary artery myocytes. Am J Physiol. 1996; 270:C321–31. [PubMed: 8772460]
132. Zhao YJ, Wang J, Rubin LJ, Yuan XJ. Inhibition of Kv and Kca channels antagonizes NO-induced relaxation in pulmonary artery. Am J Physiol. 1997; 272:H904–12. [PubMed: 9124454]
133. Yu SP, Choi DW. Ions, cell volume, and apoptosis. Proc Natl Acad Sci U S A. 2000; 97:9360–2. [PubMed: 10944207]
134. Somlyo AV, Somlyo AP. Electromechanical and pharmacomechanical coupling in vascular smooth muscle. J Pharmacol Exp Ther. 1968; 159:129–45. [PubMed: 4296170]
135. Morgan KG. Calcium and vascular smooth muscle tone. Am J Med. 1987; 82:9–15. [PubMed: 3551603]
136. Stenmark KR, Mecham RP. Cellular and molecular mechanisms of pulmonary vascular remodeling. Annu Rev Physiol. 1997; 59:89–144. [PubMed: 9074758]
137. Rubin, LJ.; Rich, S. Primary Pulmonary Hypertension. New York, NY: Marcel Dekker Inc.; 1997.

138. Golovina VA, Platoshyn O, Bailey CL, Wang J, Limsuwan A, Sweeney M, et al. Upregulated *TRP* and enhanced capacitative Ca^{2+} entry in human pulmonary artery myocytes during proliferation. Am J Physiol Heart Circ Physiol. 2001; 280:H746–55. [PubMed: 11158974]

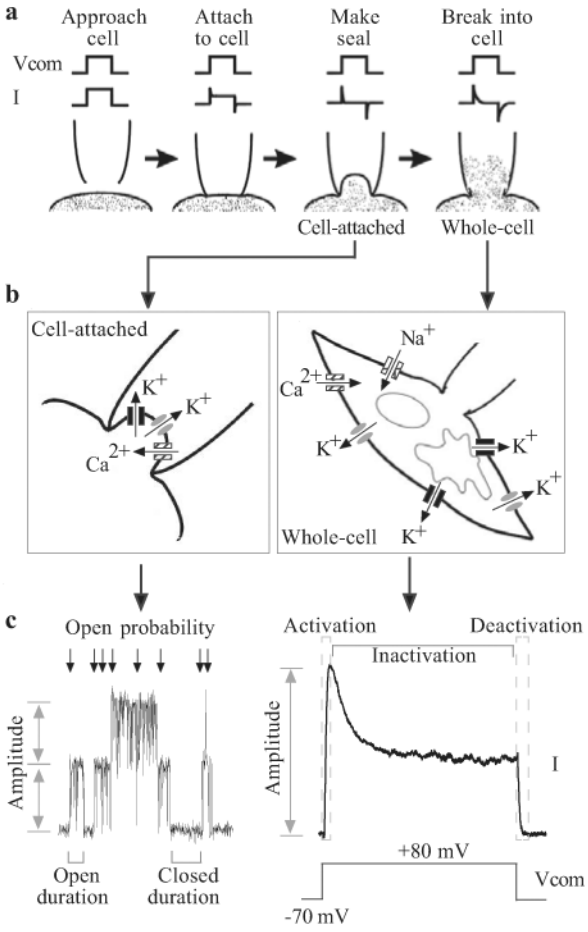

Figure 1.

Patch-clamp electrophysiology. (a) Formation of the gigaΩ seal and the subsequent cell-attached and whole-cell configurations. (b) Enhanced view of the membrane–pipette arrangements in the cell-attached and whole-cell configurations. In a cell-attached patch, unitary currents are produced by ion flux through single channels. Three different channel types are shown. In the whole-cell mode, the macroscopic current recorded is the summation of all the currents generated by similar channels throughout the cell. (c) Measured parameters. Single-channel recordings can provide information relating to the amplitude the unitary currents, the open probability of the channels and the amount of time the channel(s) spend in open (open duration) or closed (closed duration) configurations. Macroscopic currents are characterized by the current amplitude, activation, inactivation and deactivation during a pulse protocol

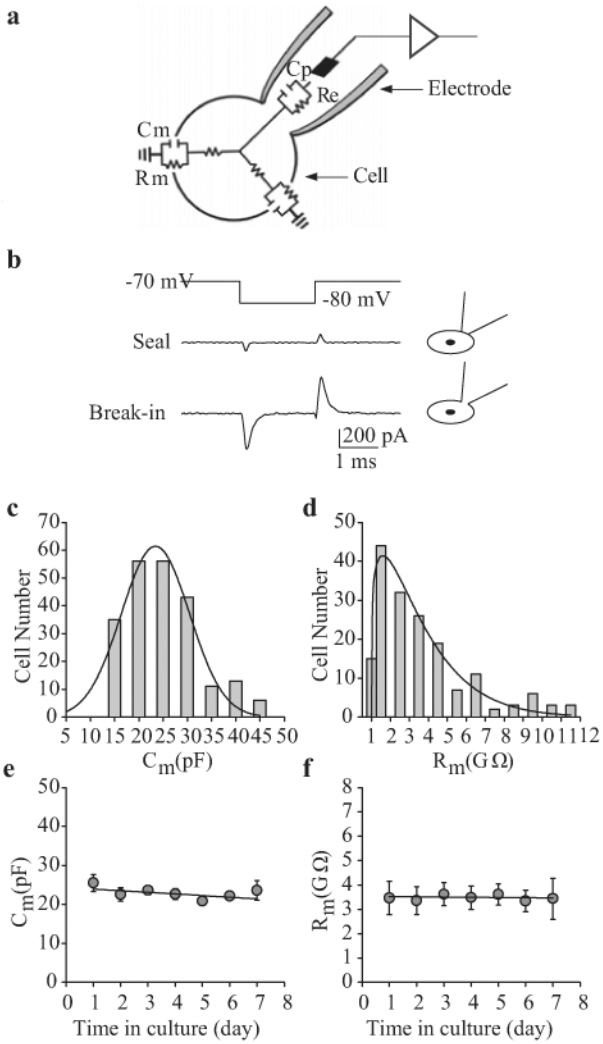

Figure 2.

Passive membrane properties of human pulmonary artery smooth muscle cells (PASMC). (a) The cell and pipette form a circuit in the whole-cell patch-clamp configuration. Membrane capacitance (C_m) and resistance (R_m) are indicators of cell size and transmembrane ion flux, respectively. (b) C_m is often used to indicate that the membrane is ruptured. In the cell-attached configuration ("Seal"), C_m, measured as the surface area under the transient spikes, is small. Upon whole-cell access ("Break-in"), C_m is greatly increased. (c and d) Frequency distribution of C_m and R_m within a cell population. (e and f) C_m (n=220) and R_m (n=171) of human PASMC do not vary over time in culture

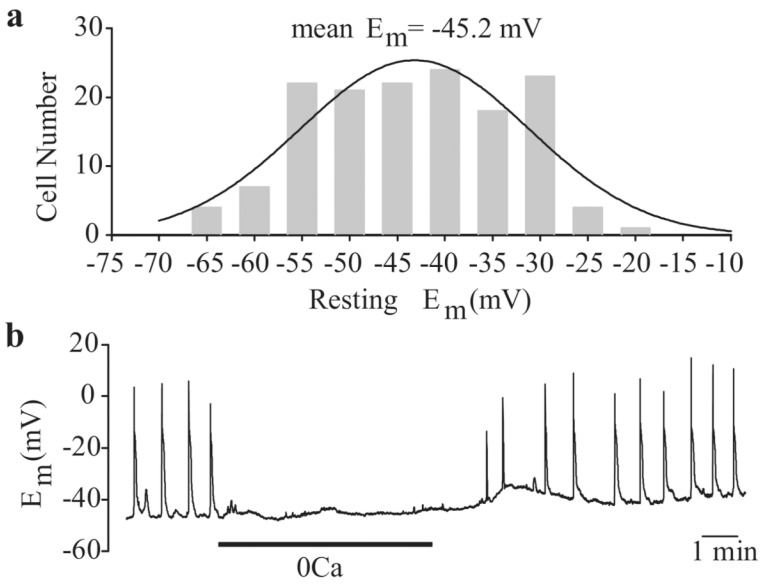

Figure 3.

Electrically active human pulmonary artery smooth muscle cells (PASMC). (a) Histogram showing the wide distribution of resting E_m in human PASMC. E_m was measured in the current clamp (I=0) mode. (b) Spontaneous action potentials recorded in human PASMC are abolished when external Ca^{2+} is removed. Electrical activity is restored upon return to normal physiological Ca^{2+} (1.8 mM)

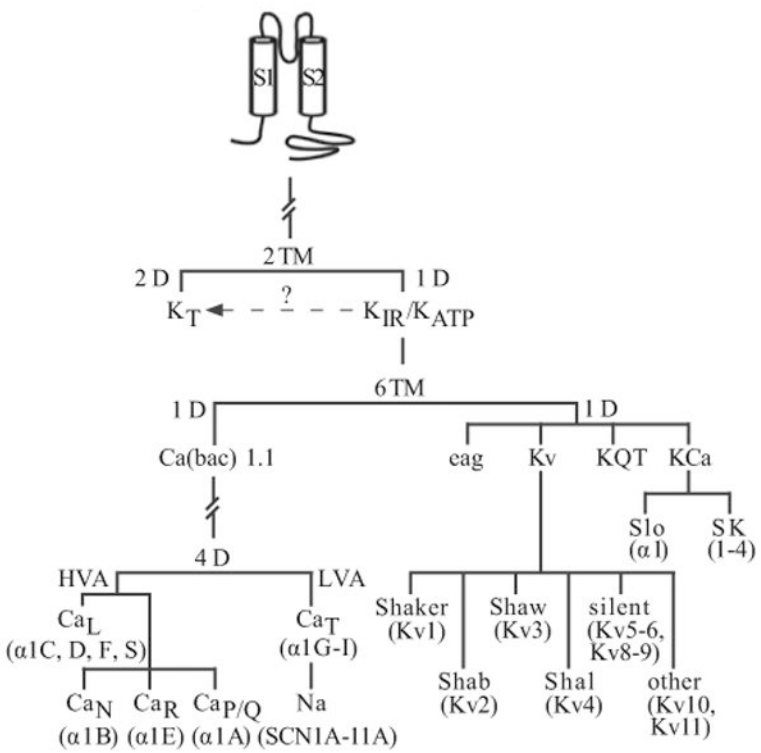

Figure 4.

Proposed phylogenetic tree depicting the evolution of voltage-dependent cation channels. Pore-forming unit isoforms representing each channel are shown in parentheses. (TM – Transmembrane domain; D – Domain; K_T – Two-pore domain K^+ channel; K_{IR} – Inward rectifier K+ channel; K_{ATP} – ATP-sensitive K^+ channel; HVA – High-voltage activated; LVA – Low-voltage activated; Kv – Voltage-gated K^+ channel; K_{QT} – Long-QT K^+ channel; Kca – Ca^{2+}-activated K^+ channel; SK – small-conductance Ca^{2+}-activated K^+ channel)

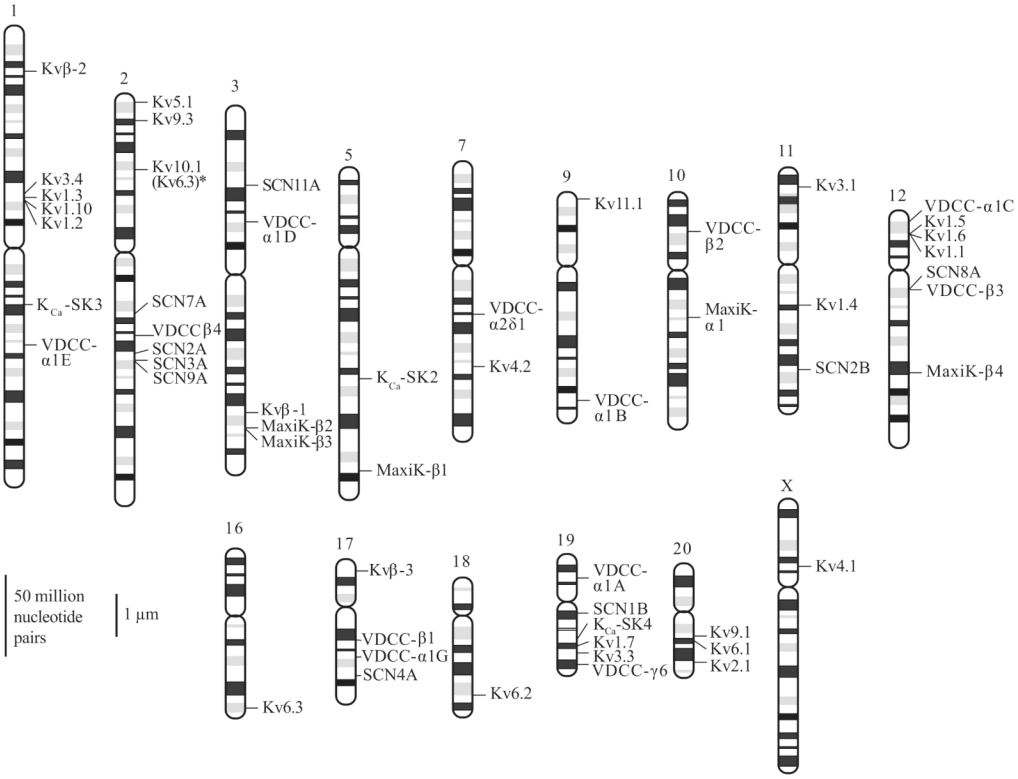

Figure 5.

Chromosomal location of ion channel genes expressed in human pulmonary artery smooth muscle cells (PASMC). All isoforms of pore-forming and regulatory subunits of Na^+, voltage-dependent Ca^{2+} channels, Kv, and Kca channels identified in human PASMC are shown. Chromosomal location is based on the primer sequences described in Table 2

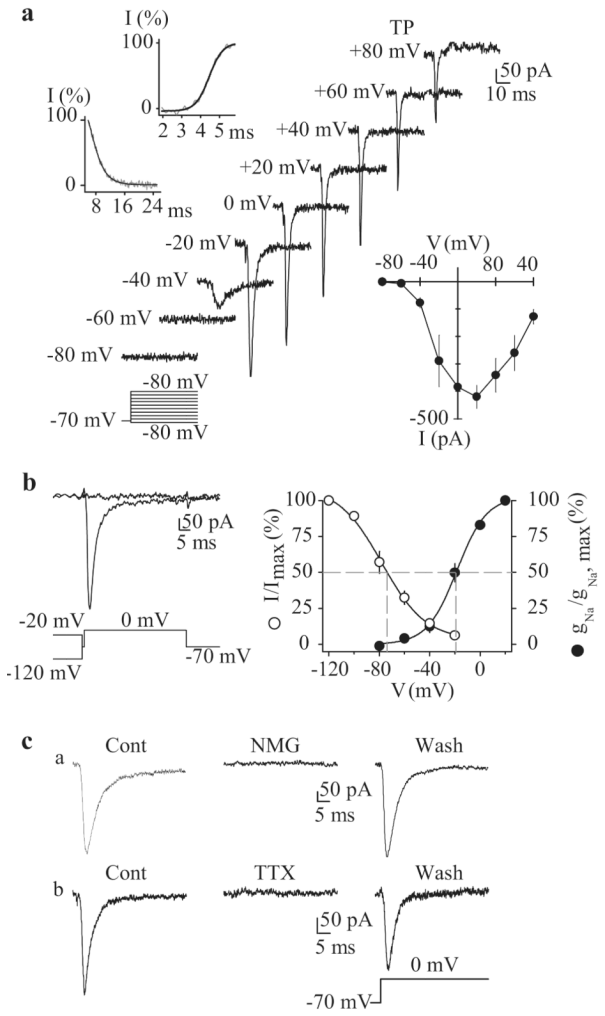

Figure 6.

Electrophysiological and pharmacological properties of voltage-gated Na^+ currents ($I_{Na(V)}$) in human pulmonary artery smooth muscle cells (PASMC). Cells are dialyzed with a Cs^+-containing pipette solution [Table 1]. (a) Representative currents were elicited by depolarizing the cell to from a holding potential of −70 mV to test potentials between −80 mV and +80 mV (protocol at bottom). *Upper left inset*: Steady-state activation and inactivation of currents occurred within <5 ms and <16 ms, respectively. *Lower right inset*: Summarized $I_{Na(V)}$ I-V relationship. (b) Currents were evoked by a step depolarization to 0 mV from different conditioning potentials (-120 mV and -20 mV) applied for 10 s prior to the test depolarization (left). Voltage-dependent steady-state availability (I/I_{max}) and normalized conductance-voltage relationship ($g_{Na}/g_{Na,\ max}$) of the peak $I_{Na(V)}$ amplitude. The I/I_{max} and $g_{Na}/g_{Na,\ max}$ curves were best fitted using exponential and Boltzman equations, respectively. (c) $I_{Na(V)}$ is completely suppressed by equimolar replacement of extracellular Na^+ with N-methyl-D-glucamine (NMG) or extracellular application of 1 μM tetrodotoxin. Currents were elicited by step depolarizations from −70 mV to 0 mV

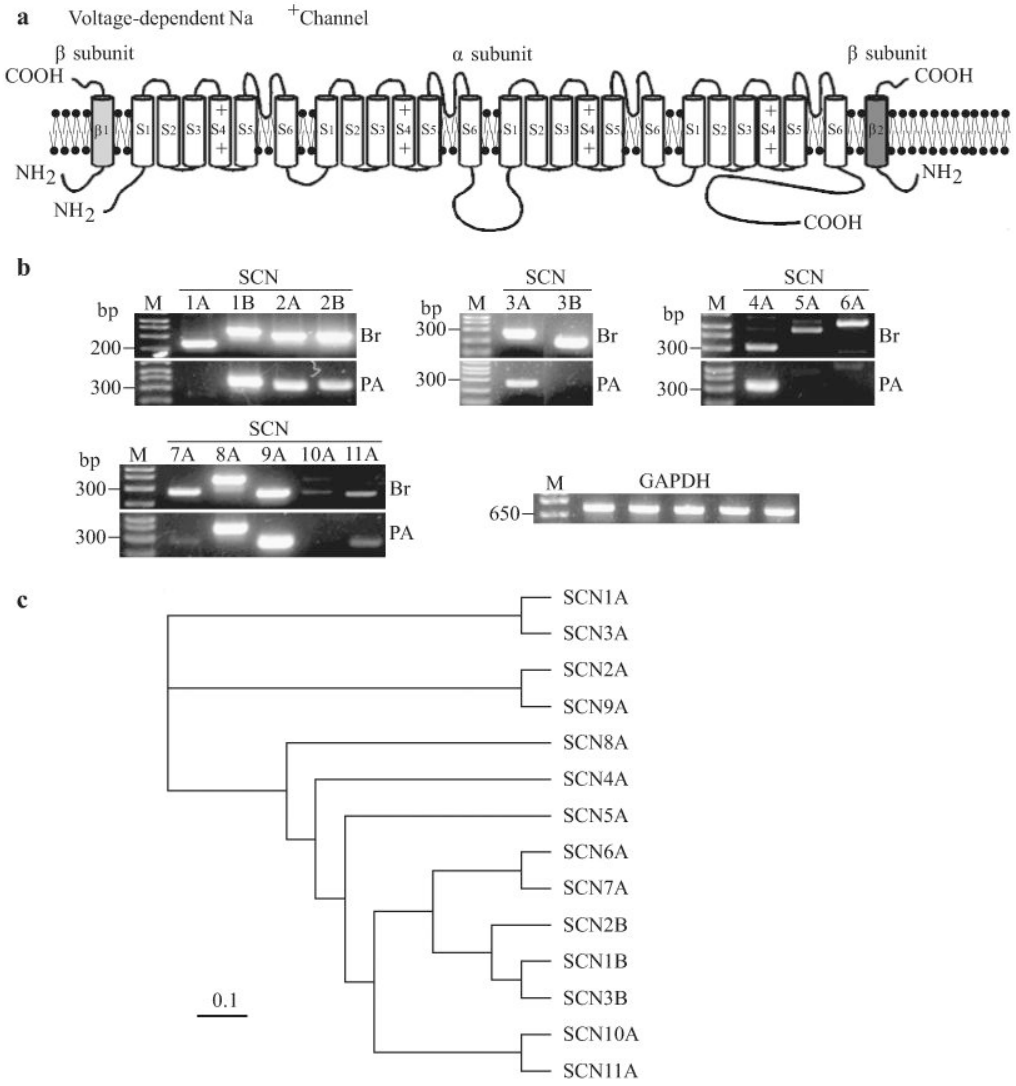

Figure 7.

Molecular identity of voltage-gated Na^+ channels in human pulmonary artery smooth muscle cells (PASMC). (a) Structural arrangement of Na^+ channel α-, β_1- and β_2-subunits. (b) The mRNA expression of cloned Na^+ channels in human brain (Br) and PASMC (PA). Polymerase chain reaction (PCR)-amplified products displayed for the transcripts of SCN2A, SCN4A, SCN5A, SCN6A and β-actin. "-RT", PCR performed with no reverse transcriptase (RT). "M", 100 bp DNA ladder. (c) A phylogenetic tree showing the inferred evolutionary relationships among different Na^+ channel genes

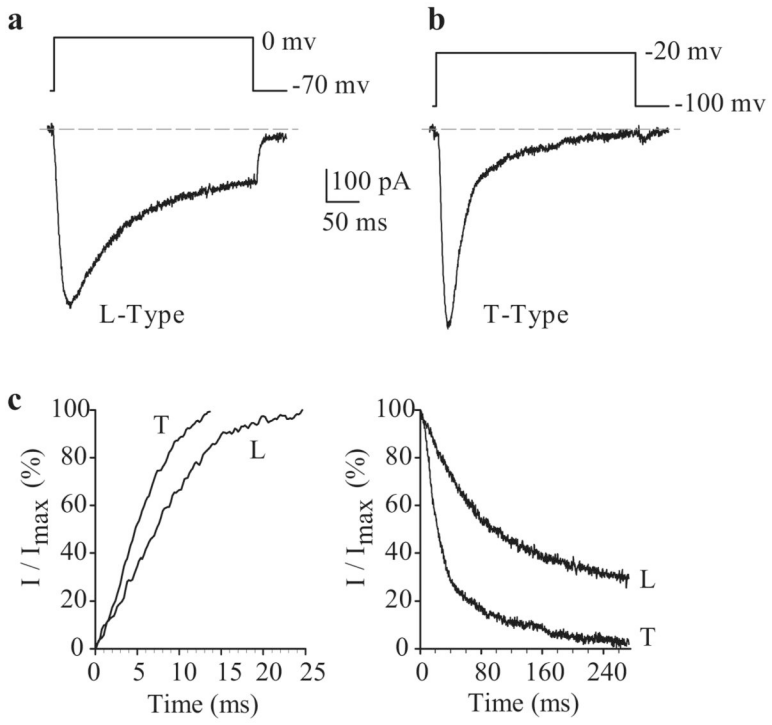

Figure 8.

Electrophysiological and pharmacological properties of L- and T-type voltage-dependent Ca^{2+} currents (I_{Ca}) in human pulmonary artery smooth muscle cells (PASMC). Cells were dialyzed with a Cs^{+}-containing pipette solution [Table 1]. (a) A representative current (L-type I_{Ca}), elicited by depolarizing a cell from a holding potential of -70 mV to 0 mV. (b) A representative current (L-type I_{Ca}), elicited by depolarizing a cell from a holding potential of -100 mV to -20 m V. (c) Activation (left) and inactivation (right) kinetics of L-type and T-type I_{Ca}

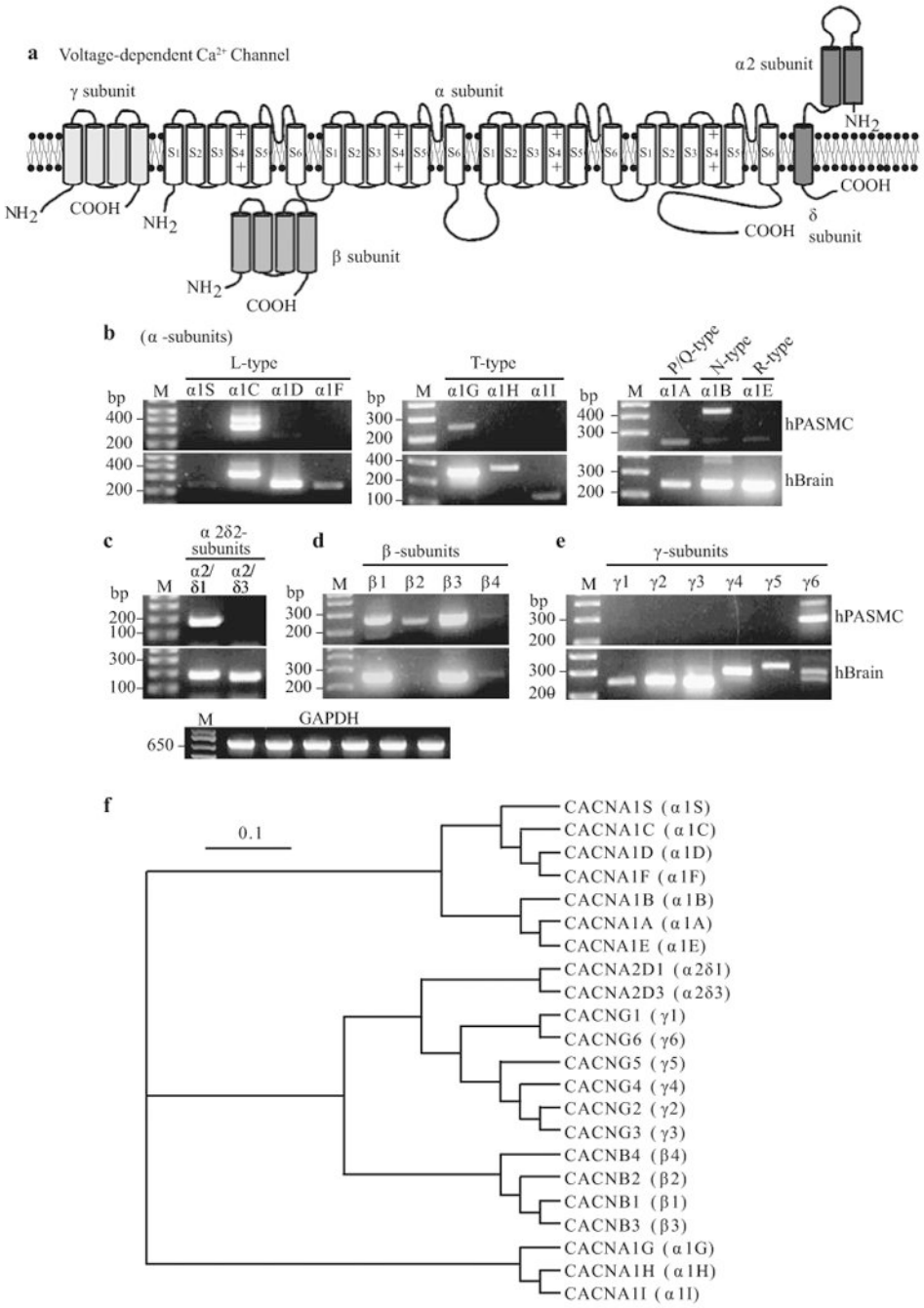

Figure 9.

Molecular identity of voltage-dependent Ca^{2+} channels (VDCC) in pulmonary artery smooth muscle cells (PASMC). (a) Structural arrangement of Ca^{2+} channel α-, β-, $\alpha_2\beta$- and γ-subunits. (b–e) The mRNA expression of α (1A-1F, 1S), $\alpha_2\delta$ (δ1 and δ3), β (1-4) and γ (1-6) subunits for L-, T-, P/Q-, N- and R-type VDCC in human PASMC (hPASMC) and brain tissues (hBrain). "M," 100 bp DNA ladder. (f) A phylogenetic tree showing the inferred evolutionary relationships among different Ca^{2+} channel genes

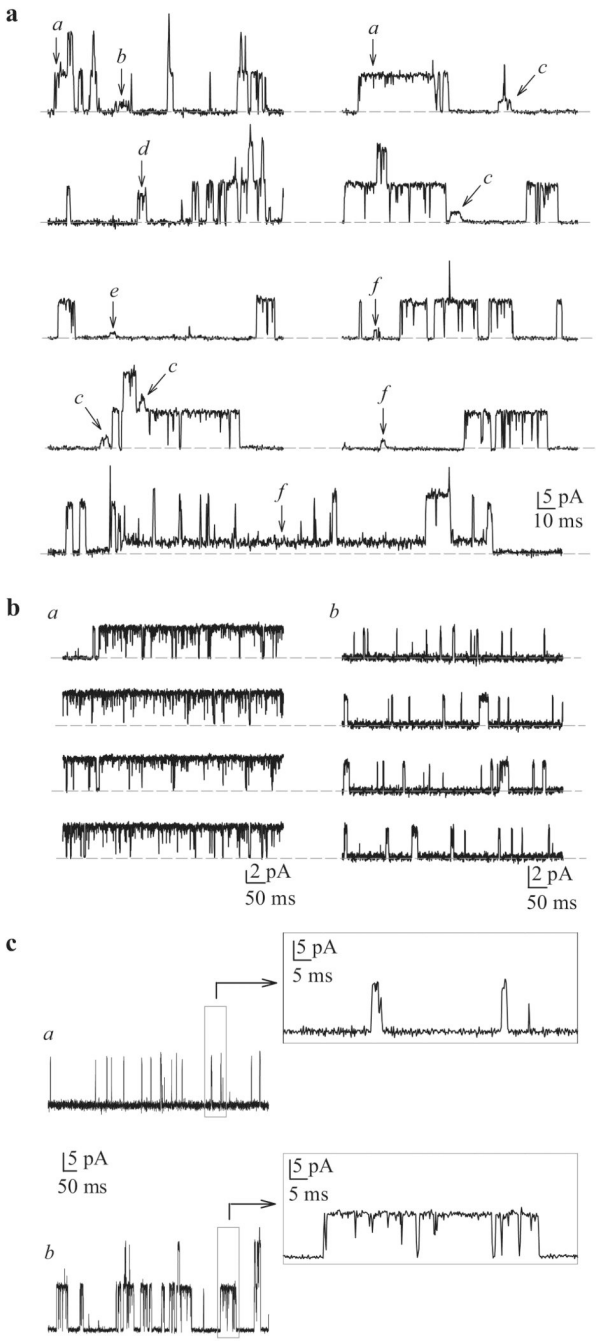

Figure 10.

Single-channel K^+ currents in cell-attached patches of human pulmonary artery smooth muscle cells (PASMC). (a) Recordings from a human PASMC showing the variability of current amplitudes (*a-f*) within the same patch. The horizontal broken line indicates the level of currents when the channels are closed. Unitary Kv (b) and Kca (c) openings can be sustained (*a*) or flickery (*b*). (c). View of flickery and sustained $i_{K(Ca)}$ on expanded time scales

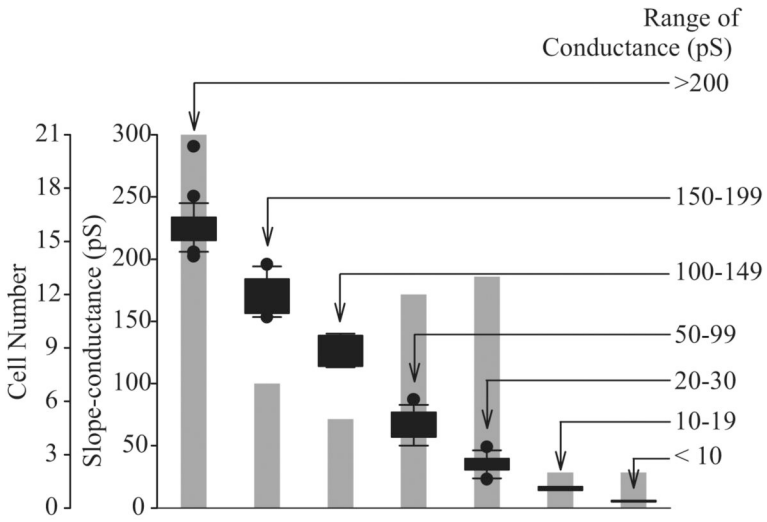

Figure 11.

Range of single-channel conductances of K^+ channels observed in human pulmonary artery smooth muscle cells (PASMC). Floating bar graph showing modes, medians and ranges of the seven conductance classes identified in human PASMC. The number of cells exhibiting particular channel conductances is indicated by the gray-shaded bars

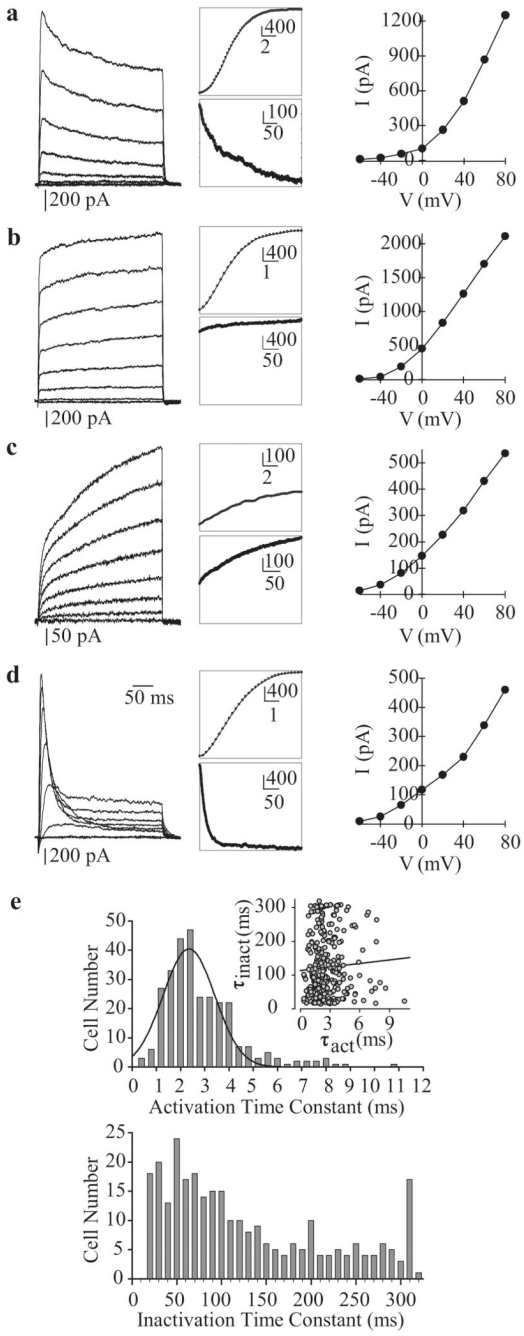

Figure 12.

Whole-cell voltage-gated K^+ (Kv) currents ($I_{K(V)}$) in human pulmonary artery smooth muscle cells (PASMC). (a–d) Four different types of Kv currents were elicited by step depolarizations from a holding potential of −70 mV to test potentials between -80 mV and +80 mV in 20 mV increments. Representative families of currents (left panels), enlarged trace segments showing steady-state activation (middle, top panels) and inactivation (middle, bottom panels) and I-V curves are presented for each type of current. (e) Activation (top) and inactivation (bottom) time constants are plotted as a function of cell number. The majority of currents activated rapidly (within 1-4 ms). The range of inactivation constants is more varied, reflecting the different current types

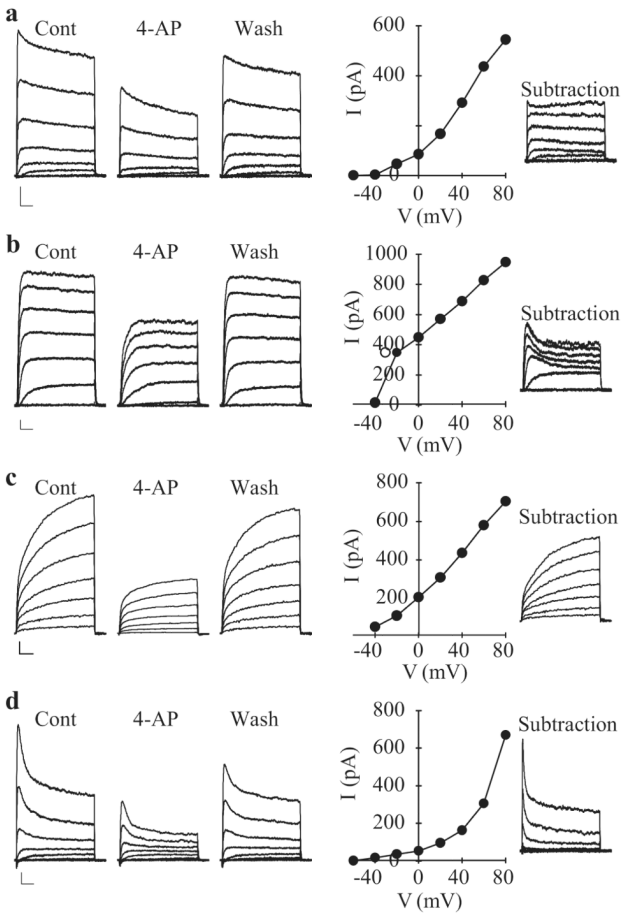

Figure 13.

Inhibitory effect of 4-amynopyridine (4-AP) on macroscopic voltage-gated K^+ (Kv) currents ($I_{K(V)}$) in pulmonary artery smooth muscle cells (PASMC). Rapidly activating and slowly inactivating (a), rapidly activating and non-inactivating (b) and rapidly activating and rapidly inactivating (c) were elicited by step depolarizations between -80 mV and +80 mV from a holding potential of -70 m V. Representative traces are shown before (Cont), during (4-AP) and after (washout) the application of 5 mM 4-AP. I-V curves of 4-AP-sensitive currents (subtraction of the currents recorded during 4-AP from the control currents) are presented in the middle panels for each current type. The 4-AP-sensitive current components depicted to the right were obtained by digital subtraction (Cont − 4-AP)

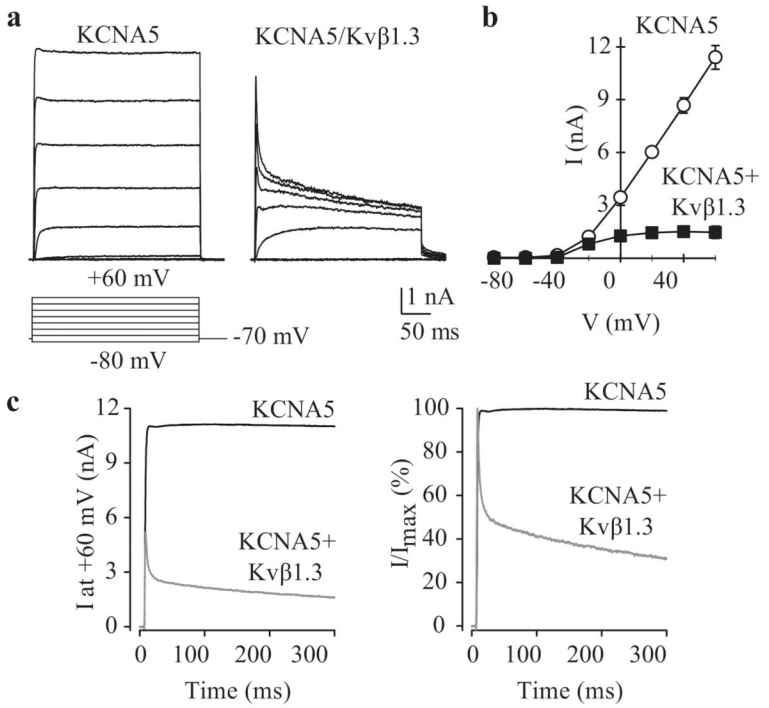

Figure 14.

Co-transfection of Kvβ-subunits affects KCNA5 channel kinetics. HEK-293 cells were transfected with wild-type KCNA5 alone (KCNA5) or in the presence of Kvβ1.3-HA (KCNA5/Kvβ1.3). Representative current recordings (a) and I-V curves (b) are shown (pulse protocol, lower panel). (c) Averaged currents (*left*) and normalized currents (*right*) at +60 mV in cells transiently transfected with WT KCNA5 alone (KCNA5) or WT KCNA5 + Kvβ1.3-HA (KCNA5/Kvβ1.3)

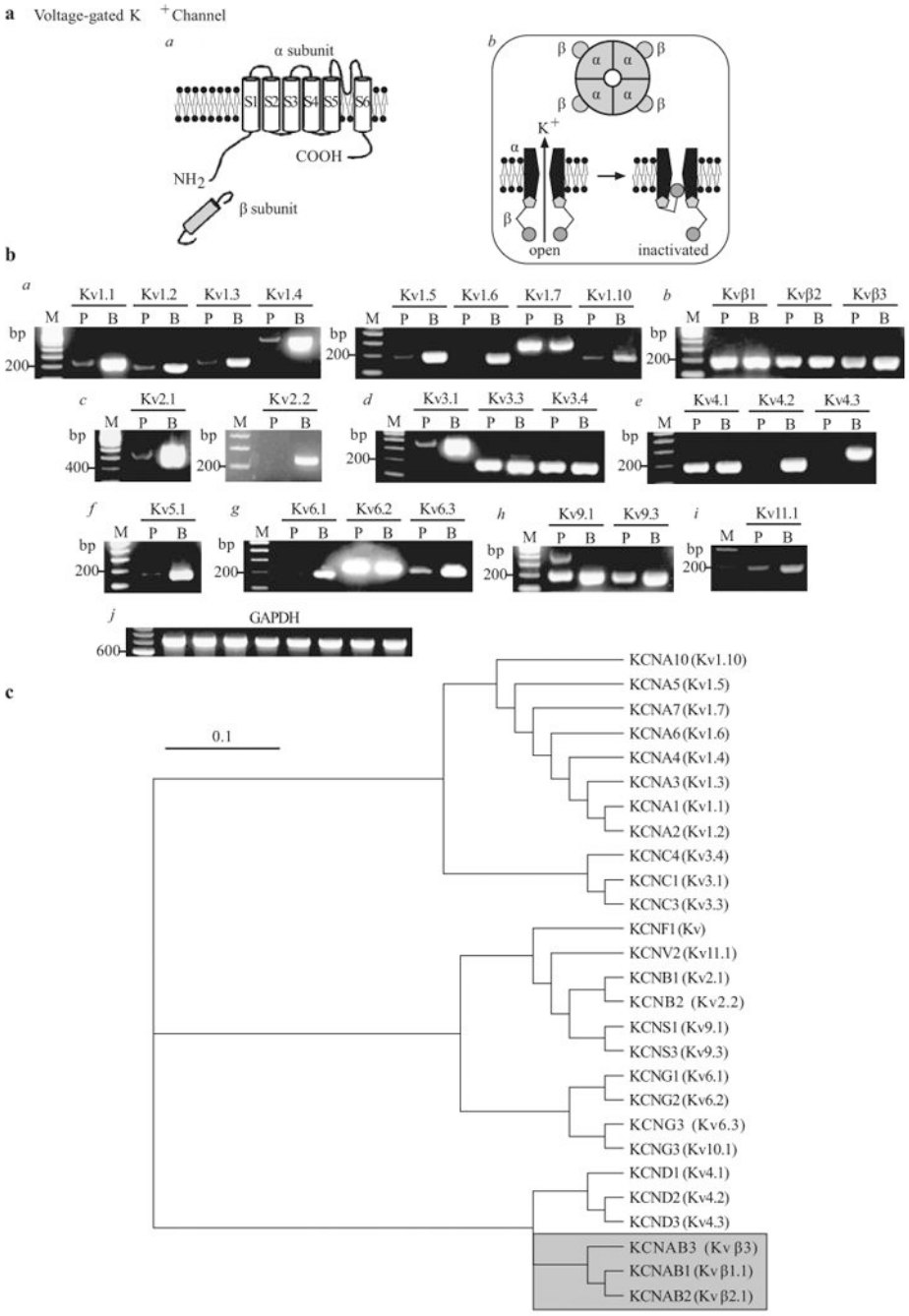

Figure 15.

Molecular identity of voltage-gated K^+ (Kv) channels in pulmonary artery smooth muscle cells (PASMC). (a) Structural arrangement of Kv channel α- and β-subunits (*a*), the tetrameric association of α–subunits (*b*) and the ball-and-chain inactivation mechanism for $I_{K(V)}$ (b). (b) The mRNA expression of reverse transcriptase-polymerase chain reaction products using Kv1 (*a*), Kvβ (*b*), Kv2 (*c*), Kv3 (*d*), Kv4 (*e*), Kv5 (*f*), Kv6 (*g*), Kv9 (*h*) and Kv11 (*i*) primers in human PASMC (P) and brain (b) tissues. "M," 100 bp DNA ladder. (c) A phylogenetic tree showing the inferred evolutionary relationships among different Kv channel genes

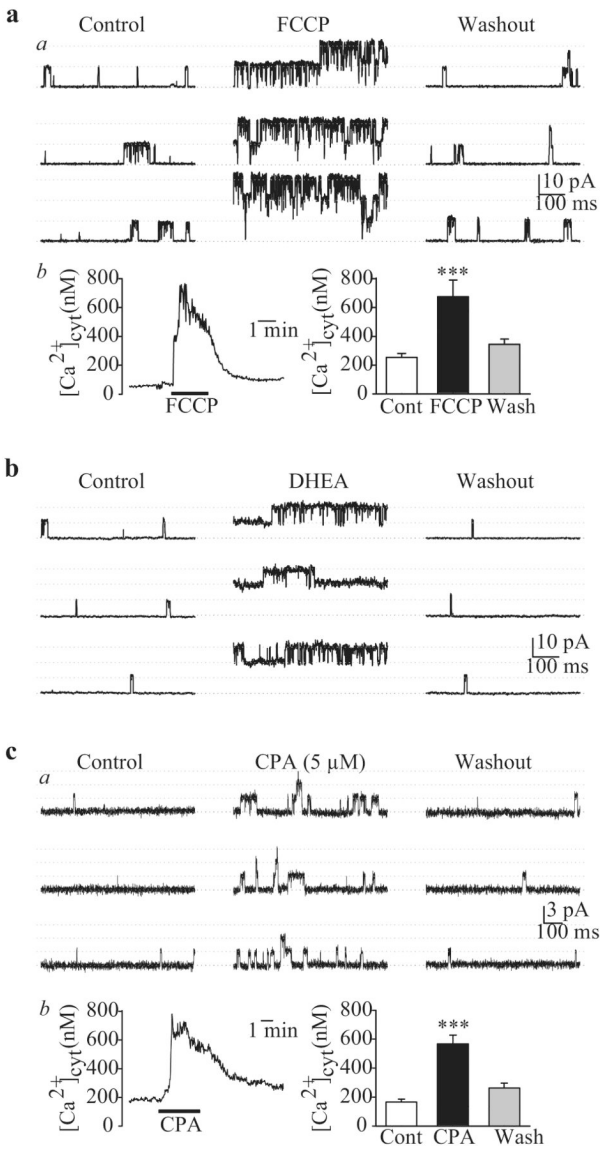

Figure 16.

Single-channel Ca^{2+}-activated K^+ (Kca) currents ($i_{K(Ca)}$) in cell-attached membrane patches of human pulmonary artery smooth muscle cells (PASMC). (a) FCCP (5 μM) enhances large-amplitude $i_{K(Ca)}$ open probability (P_{open}) (*a*) by causing a transient $[Ca^+]_{cyt}$ (*b*) increase. (b) dihydroepiandrosterone (0.1 mM) also enhances the large-amplitude $i_{K(Ca)}$ P_{open}. (c) Cyclopiazonic acid (5 μM), an inhibitor of sarcoplasmic reticulum (SR) Ca^{2+} pump, increases the activity of a smaller amplitude $i_{K(Ca)}$ (*a*) by causing SR Ca^{2+} release from the SR to the cytosol (*b*)

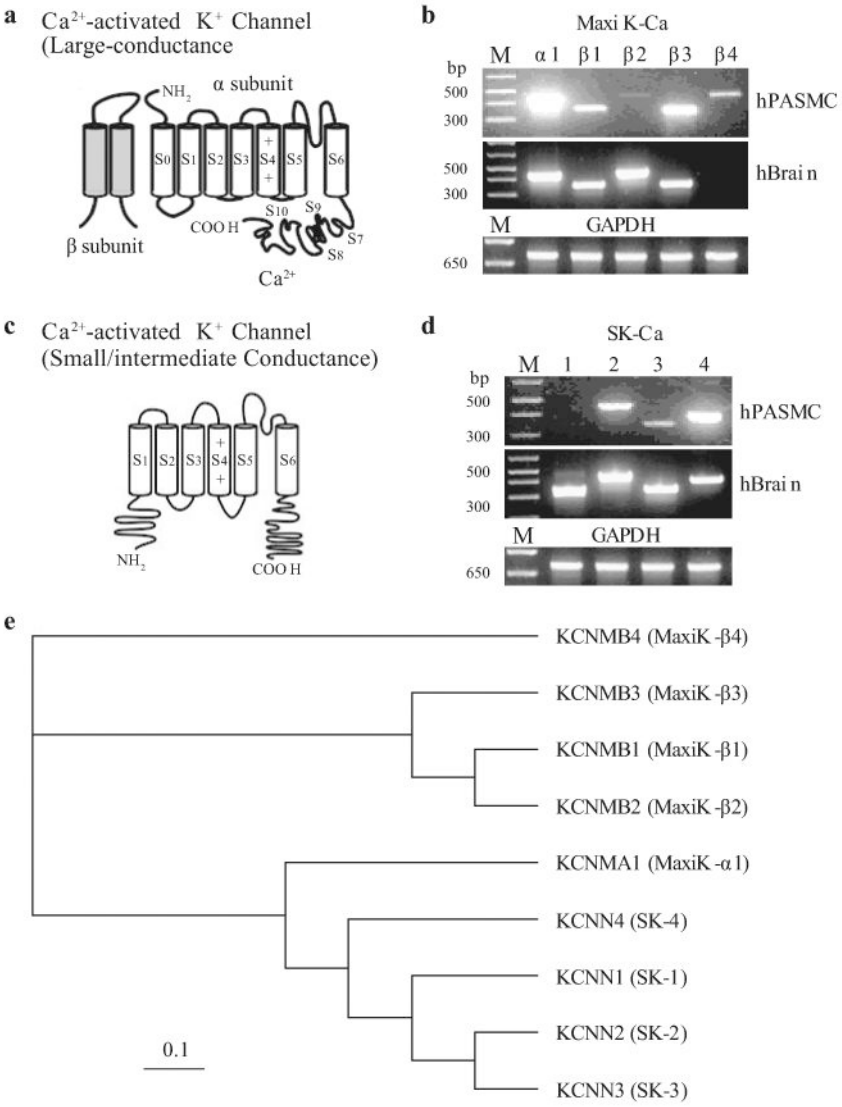

Figure 17.

Molecular identity of Ca^{2+}-activated K^+ (Kca) channels in human pulmonary artery smooth muscle cells (PASMC). (a) Structural arrangement of Kca channel α- and β-subunits. The putative binding site for Ca^{2+} is shown on the C-terminal region of the α-subunit. (b–d) The mRNA expression of reverse transcriptase-polymerase chain reaction products for maxi Kca channel α1 and β1-4 subunits (b) and small- (SK1-3) and intermediate- (SK4) channels (c and d) are shown in human PASMC and brain tissues. “M,” 100 bp DNA ladder. (e) A phylogenetic tree showing the inferred evolutionary relationships among different Kca channel genes

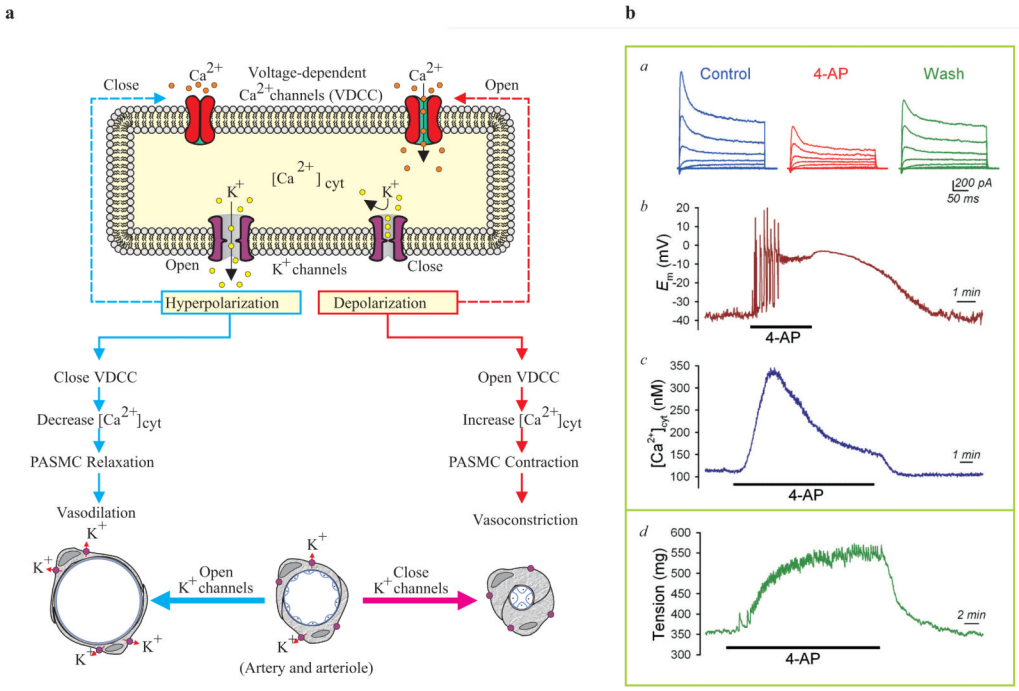

Figure 18.

Inhibition of K^+ channels causes membrane depolarization and causes pulmonary vasoconstriction. (a) Closure of K^+ channels in pulmonary artery smooth muscle cells (PASMC) causes membrane depolarization, which subsequently opens voltage-dependent Ca^{2+} channels (VDCC), enhances Ca^{2+} influx, increases $[Ca^{2+}]_{cyt}$ and induces pulmonary vasoconstriction. Opening of K^+ channels, on the other hand, causes membrane hyperpolarization (close to the K^+ equilibrium potential), decreases VDCC activity and causes pulmonary vasodilation. (b) Representative records of whole-cell K^+ currents (*a*), membrane potential (E_m, *b*) and $[Ca^{2+}]_{cyt}$ (*c*) in PASMC before (control), during (4-AP) and after (wash) extracellular application of 5 mM 4-amynopyridine (4-AP), an inhibitor of Kv channels. (*d*) A representative record of tension measurement in an isolated mouse pulmonary arterial ring before, during and after 4-AP treatment is shown

Table 1

Ionic composition of extracellular and intracellular solutions used for measurement of various ion channel currents

Current Type	Na^+ mM	Ca^{2+} mM	K^+ mM	Mg^{2+} mM	Cl^- mM	Cs^+ mM	ATP mM	EGTA mM	Glu mM	HEPES mM	pH
I_{Na} (whole cell)											
Bath	141	-	4.7	3	151.7	-	-	1	10	10	7.4
Pipette	10	-	-	4	143	135	5	10	-	10	7.2
I_{Ca} (whole cell)											
Bath	110	20	4.7	1.2	157.1	-	-	-	10	10	7.4
Pipette	10	-	-	4	143	135	5	10	-	10	7.2
$I_{K(V)}$ (whole cell)											
Bath	141	-	4.7	3	151.7	-	-	1	10	10	7.4
Pipette	10	0	135	4	143	-	5	10	-	10	7.2
$I_{K(Ca)}$ (whole cell)											
Bath	141	1.8	4.7	1.2	151.7	-	-	-	10	10	7.4
Pipette	10	0 (8.8)	135	4	143	-	5	- (10)	-	10	7.2
$I_{K(Ca)}$ (cell attached)											
Bath	141	1.7	4.7	1.2	151.7	-	-	-	10	10	7.4
Pipette	10	-	125	4	129	-	5	0.1	-	10	7.2
$I_{K(V)}$ (cell attached)											
Bath	141	1.8	4.7	1.2	151.7	-	-	-	10	10	7.4
Pipette	5	0	137	1.2	143.2	-	5	0.1	0	10	7.2

Table 2
Oligonucleotide sequences of the RT-PCR primers

Standard names (Accession no.)*	Size (bp)	Predicted sense/antisense	Location (nt)	Gene (chromosome)
Voltage-gated Na^+ channels				
SCN2A	629	5′-ACATCTGTGTGAAGGCTGGTAG-3′/	1157-1179	2q23-q24
(X65361)		5′-CAGTAAGGACTGGTGTGGAGAA-3′	1763-1785	
SCN4A	684	5′-GCCGTTCAACGACACCAACACC-3′/	932-954	17q23.1-q25.3
(M81758)		5′-GATGTGTCCAGGCTGCCATTGC-3′	1593-1615	
SCN5A	466	5′ -AGAAGATGGTCCCAGAGCAATG-3′/	1647-1669	3p21
(M77235.1)		5′-CTCGAAGCCATCTACACACGGA-3′	2090-2112	
SCN6A	507	5′-CAGATGAGGCCAAGACCATACA-3′/	1422-1444	2q21-q23
(M91556)		5′-ATCGAAGAAGAGCCATTCCTGC-3′	1906-1928	
β-actin	661	5′-GACGGGGTCACCCACACTGTGCCCATCTA-3′/	2134-2162	7p22-p12
(M10277)		5′-CTAGAAGCATTTGCGGTGGACGATGGAGG-3′	2971-3000	
β-actin	314	5′-CACTCTTCCAGCCTTCCTTC-3′/	820-840	7p22-p12
(X00351)		5′-CTCGTCATACTCCTGCTTGC-3′	1113-1133	
Voltage-gated Ca^{2+} channels				
L-type				
α_{1S}	246	5′-GGGAGCGAGGAGAGTAATCC-3′/	46-65	1q32
(NM_000069)		5′-CTCAGGAACTGGCTTCTTGG-3′	272-291	
α_{1C}	357	5′-TCTTTCACCCCAATGCCTAC-3′/	1875-1894	12p13.3
(NM_000719		5′-CCTCCTGGTTGTAGCAGGTC-3′	2212-2231	
α_{1D}	258	5′-GCCAGATTGGTTGACACAGA-3′/	1819-1838	3p14.3
(XM_003238)		5′-CAGTGCCTGGTCACTTTGAA-3′	2057-2076	
α_{1F}	251	5′-CTACTTCCTGGGATCCGACA-3′/	863-882	Xp11.23
(NM_005183		5′-ACACCCAGGGCAGTTCATA-3′	1095-1113	
T-type				
α_{1G}	250	5′-TTCCCAAAGATGCACCTCAT-3′/	494-513	17q22
(AF029229)		5′-TGTGCCTGGGTACTTGACTG-3′	724-743	
α_{1H}		5′-ACCGTGTTCCAGATCCTGAC-3′/	3144-3163	22q13.1
(NM_021096)		5′-TGAAGAGCACATAGTTGCCG-3′	3251-3270	
α_{1I}	270	5′-CCGTGGTTTGAATGTGTCAG-3′/	235-254	22q13.1
(XM_010005)		5′-GTCCAGGGAGTACTCGACCA-3′	485-504	
N-type				
α_{1B}	254	5′-CCCAGGCAGTGGAAGAAATA-3′/	2041-2060	9q34
(XM_015804)		5′-TGCTCCTGGAAGGTGATGAT-3′	2275-2294	
P/Q-type				
α_{1A}	250	5′-TTGCCCTACAGAAAGCCAAG-3′/	2458-2477	19p13.2-p13.1
(XM_051369)		5′-TCCAAGTGCGTCTTCATGTC-3′	2688-2707	
R-type				
α_{1E}	253	5′-GTGGCAAGTTACATCGAGCA-3′/	988-1007	1q25-q31

Standard names (Accession no.)*	Size (bp)	Predicted sense/antisense	Location (nt)	Gene (chromosome)
(XM_001815)		5′-CAATTCCAGGTGGCTCCTAA-3′	1221-1240	
$\alpha_2\delta_1$	178	5′-AGTGGATGGCCTGTGAAAAC-3′/	1231-1250	7q21-q22
(XM_167505)		5′-ACAAGTCCCAGTTCCAATGC-3′	1389-1408	
$\alpha_2\delta_3$	167	5′-CCTGTGCCAACAAAGGATTT-3′/	555-574	3p21.1
(XM_035446)		5′-CTTTTGTGCCTGAGGGAGAG-3′	702-721	
β_1	253	5′-CTGGCTAAGCGCTCAGTTCT-3′/	976-995	17q21-q22
(XM_054993)		5′-GGGACTTGATGAGCCTTTGA-3′	1209-1228	
β_2	241	5′-CCACAACCACAGAGACGAGA-3′/	2097-2116	10p12
(NM_000724)		5′-AACACAAAAGGGCAAAACTC-3′	2318-2337	
β_3	248	5′-AGGAGATCTGGGAACCCTTC-3′/	406-425	12q13
(XM_028766)		5′-GTGACTCGGGTGATGGAGAT-3′	634-653	
β_4	262	5′-CGCACCCTGAGAGTCTTTGT-3′/	342-361	2q22-q23
(AF216867)		5′-CCACCTGGACTCGACACAC3′	585-603	
γ_1	250	5′-GATTTGTACCAAGCGCATCC-3′/	236-255	17q24
(XM_008262)		5′-TCGCAGCAGATAGTCCCTCT-3′	466-485	
γ_2	249	5′-GGCTGTTTGATCGAGGTGTT-3′/	5-24	22q13.1
(NM_006078)		5′-TGCATCCTCTGGGAAGTGAT-3′	242-261	
γ_3	259	5′-CCTTGGGGGAAGTGTACAGA-3′/	1327-1346	1612-p13.1
(NM_006539)		5′-CAAGGAGGGAAGAATGTGGA-3′	1566-1585	
γ_4	299	5′-CTACAGCCGCAAGAACAACA-3′/	407-426	17q24
(NM_014408)		5′-AAGGAGAAGAGGAAGACGCC-3′	686-705	
γ_5	337	5′-CGATGAGATGCTCAACAGGA-3′/	471-490	17q24
(AF361351)		5′-CTGATCATAGTCGGGGCACT-3′	788-807	
γ_6	271	5′-TTGGGGTGCCTCTGTATCAT-3′/	460-479	19q13.4
(AF361352)		5′-GCAGTGTGAGCAGCAGAAAG-3′	711-730	
Voltage-gated K^+ channels				
Kv1.1 (KCNA1)	258	5′-CGGGGTCATCCTGTTTTCTA-3′/	1005-1024	12p13
(NM_000217)		5′-CCCTCAGTTTCTCGGTGGTA-3′	1243-1262	
K_v1.2 (KCNA2)	200	5′-ATGAGAGAATTGGGCCTCCT-3′/	986-1005	1p13
(NM_004974)		5′-CCCACTATCTTTCCCCCAAT-3′	1166-1185	
K_v1.3 (KCNA3)	259	5′-TCTGCCTATGCCCTTGTTTT-3′/	1711-1730	1p21-p13.3
(NM_002232)		5′-TTCCTCCCAGGATGTACTGC-3′	1950-1969	
K_v1.4 (KCNA4)	571	5′-TGGCGGCTACAGTTCAGTC-3′/	1640-1658	11q13.4-q14.1
(NM_002233)		5′-ATCATTCAACAACCCACCAT-3′	2191-2210	
K_v1.5 (KCNA5)	201	5′-ACTTGCGGAGGTCCCTTTAT-3′/	2013-2032	12p13
(NM_002234)		5′-GGAGGGAGGAAAGGAGTGAA-3′	2194-2213	
K_v1.6 (KCNA6)	197	5′-CAGAGGAATCGTGTTGCAGA-3′/	3380-3399	12p13
(NM_002235)		5′-TGCCCATAAAATGGGAAGAA-3′	3557-3576	
K_v1.7 (KCNA7)	300	5′-CTTCCAGGGGCATGTTATTTTA-3′/	2254-2275	19q13.3
(NM_031886)		5′-CTCAATGGAACTCAATTCAGCA-3′	2532-2553	

Standard names (Accession no.)*	Size (bp)	Predicted sense/antisense	Location (nt)	Gene (chromosome)
K_v1.10 (KCNA10)	201	5′-TGGGGTTGCTCATCTTCTTT-3′/	1124-1143	1p13.1
(NM_005549)		5′-CACACAGAGTGCCCACAATC-3′	1305-1324	
Kvβ1 (KCNAB1)	197	5′-AGGCTGCAGCTCGAGTATGT-3′/	701-720	3q26.1
(NM_003471)		5′-ACCGGTGGGATCATATTGAA-3′	878-897	
Kvβ2 (KCNAB2)	195	5′-TGGGCAATAAACCCTACAGC-3′/	1242-1261	1p36.3
(NM_003636)		5′-CAGCGACTTGGGAGATCATT-3′	1417-1436	
Kvβ3 (KCNAB3)	200	5′-GTGGTGTTCGGGTATCCTGT-3′/	257-276	17p13.1
(NM_004732)		5′-TGATCTCCTCCAACCTTTGC-3′	437-456	
K_v2.1 (KCNB1)	383	5′-ACAGAGCAAACCAAAGGAAGAAC-3′/	1656-1678	20q13.2
(NM_004975)		5′-CACCCTCCATGAAGTTGACTTTA-3′	2016-2038	
K_v3.1 (KCNC1)	387	5′-GGAGGCCTTCCTTACCTACATC-3′/	791-812	11p15
(NM_004976)		5′-CCTATCCTCTCGGCGTAGTAGA-3′	1156-1177	
K_v3.3 (KCNC3)	199	5′-TGCTGCTCATCATCTTCCTG-3′/	1641-1660	19q13.3-q13.4
(NM_004977)		5′-GACCACGTCTTGGGGTACAT-3′	1820-1839	
K_v3.4 (KCNC4)	196	5′-CTACCTGGAGGTGGGACTGA-3′/	1131-1150	1p21
(NM_004978)		5′-CAGGGCCAGGAAGATGATAA-3′	1307-1326	
K_v4.1 (KCND1)	199	5′-GAGAAGACAACGTGCCATGA-3′/	1456-1475	Xp11.23-p11.3
(NM_004979)		5′-TGACTGAGGCAGTGGAGTTG-3′	1635-1654	
K_v4.2 (KCND2)	201	5′-GCCAATGTGTCAGGAAGTCA-3′/	1857-1876	7q31-q32
(NM_012281)		5′-TTCTGGGGTGGTTACTGGAG-3′	2038-2057	
K_v4.3 (KCND3)	275	5′-CATGGCCATCATCATCTTTG-3′/	1465-1484	1p13.3
(NM_004980)		5′-CCCTGCGTTTATCAGCTCTC-3′	1720-1739	
K_v5.1 (KCNF1)	195	5′-GCCAGCGACGACATAGAGAT-3′/	303-322	2p25
(NM_002236)		5′-CGGGTCCCTGTCAAAGTAGA-3′	478-497	
K_v6.1 (KCNG1)	191	5′-CTACTGGTGGGCTGTCATCA-3′/	1242-1261	20q13
(NM_002237)		5′-TCACCCTCTCTTGCTCCTGT-3′	1413-1432	
K_v6.2 (KCNG2)	254	5′-CTGCTGCTGCTGTTCCTCTG-3′/	347-366	18q22-q23
(NM_012283)		5′-AAAGGTGTGGAAGATGGAGGT-3′	581-601	
K_v6.3 (KCNG3)	227	5′-TGCATAGGTTGGTTCACTGC-3′/	682-701	16q24
(NM_133329)		5′-GGCAAGCTTAATCACCCAAA-3′	890-909	
(Identical gene to K_v10.1)				
K_v9.1 (KCNS1)	202	5′-ATACCAGCCCTTCTGCACAC-3′/	4234-4253	20q12
(NM_002251)		5′-AGGCCAGATGATTCCCTCTT-3′	4416-4435	
K_v9.3 (KCNS3)	200	5′-CAGTGAGGATGCACCAGAGA-3′/	1652-1671	2p24
(NM_002252)		5′-TTGCTGTGCAATTCTCCAAG-3′	1832-1851	
K_v10.1 (KCNG3)	227	5′-TGCATAGGTTGGTTCACTGC-3′/	682-701	2p21
(AF-348982)		5′-GGCAAGCTTAATCACCCAAA-3′	890-909	
(Identical gene to K_v6.3)				
K_v11.1	210	5′-CCTTCCTCTGCATTGCTTTT-3′/	1425-1444	9p24.2
(NM_133497.1)		5′-CTTGTCTTGGGGTGAGCTGT-3′	1615-1634	

Standard names (Accession no.)*	Size (bp)	Predicted sense/antisense	Location (nt)	Gene (chromosome)
Voltage-dependent Ca^{2+}-activated K^+ channels				
MaxiKca-α1	442	5′-CTACTGGGATGTTTCACTGGTGT-3′/	2210-2232	10q22
(NM_002247)		5′-TGCTGTCATCAAACTGCATA-3′	2634-2653	
MaxiKca-β1	363	5′-TCTACTGCTTCTCCGCAC-3′/	557-574	5q34
(NM_004137)		5′-GAGCAGGCAATGACTTCA-3′	902-919	
MaxiKca-β2	449	5′-GGGACTGGCTATGATGGT-3′/	502-519	3q26.2-q27.1
(NM_005832)		5′-GTGAATGGAACAGCACGTTG-3′	931-950	
MaxiKca-β3	351	5′-GCTCAACAGTGCTCTGGACA-3′/	1013-1032	3q26.3-q27.1
(NM_014407)		5′-TGGCCACCGTCTTAAGATTT-3′	1344-1363	
MaxiKca-β4	300	5′-CTGAGTCCAACTCTAGGGCG-3′/	612-631	12q14.1-q15
(NM_014505)		5′-TGGTCAGGACCACAATGAGA-3′	892-911	
Kca-SK1	357	5′-CTTCCTCTCCATTGGCTACG-3′/	1301-1320	19p13.1
(NM_002248)		5′-TTCCCTTGCTCGATCTTCAC-3′	1638-1657	
Kca-SK2	451	5′-CAAGCAAACACTTTGGTGGA-3′	1880-1899	5q22.3
(NM_021614)		5′-TGTTCAGGTTCCCAGGATTC-3′	2311-2330	
Kca-SK3	349	5′-CTTGATCATCGCCTACCACA-3′/	1344-1363	1q21.3
(NM_002249)		5′-GCGGGTGTTGAAGTTGATCT-3′	1673-1692	
Kca-SK4	399	5′-GCCCTGGAGAAACAGATTGA-3′/	1567-1586	19q13.2
(NM_002250)		5′-AGAGCTGGAGGTCGTCCATA-3′	1946-1965	

* The accession numbers in GenBank for the sequence used in designing the primers

Table 3

Biophysical properties and molecular identities of voltage-dependent cation channels expressed in human PASMC

Types of currents	Activation threshold	Blocked by (EC_{50})	Gene transcripts identified
I_{Na}	-34 mV	Tetrodotoxin	SCN5A
			SCN6A
I_{Ca}	-24 mV (HVA)	Nickel	L-type (α_{1C}, α_{1D})
	-50 mV (LVA)	Nifedipine	T-type (α_{1G})
			P/Q-type (α_{1A})
			N-type (α_{1B})
			R-type (α_{1E})
			$\alpha_2\delta_1$
			β_1, β_2, β_3, β_4
			γ_6
$I_{K(V)}$	-55 mV	4-AP	K_v1.1, 1.2, 1.3, 1.4, 1.5, 1.6, 1.7,
			1-10
			K_v2.1
			K_v3.1, 3.3, 3.4
			K_v4.1, 4.2
			K_v5.1
			K_v6.1, 6.2, 6.3
			K_v9.1, 9.3
			K_v10.1
			K_v11.1
			$K_v\beta$1, β2, β3
$I_{K(Ca)}$	-25 mV	Iberiotoxin	Maxi-Kca α_1
		Charybdotoxin	Maxi-Kca β1, β2, β3, β4
			SK2, 3, 4